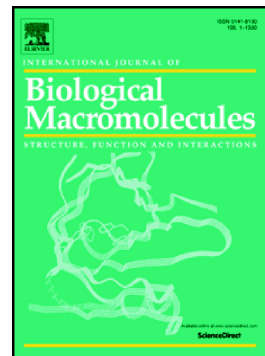# Journal Pre-proof

Properties of scaffolds prepared by fused deposition modeling of poly(hydroxyalkanoates)

Adriana Kovalcik, Leire Sangroniz, Michal Kalina, Katerina Skopalova, Petr Humpolíček, Maria Omastova, Norbert Mundigler, Alejandro J. Müller

Please cite this article as: A. Kovalcik, L. Sangroniz, M. Kalina, et al., Properties of scaffolds prepared by fused deposition modeling of poly(hydroxyalkanoates), *International Journal of Biological Macromolecules* (2020), https://doi.org/10.1016/j.ijbiomac.2020.06.022

This is a PDF file of an article that has undergone enhancements after acceptance, such as the addition of a cover page and metadata, and formatting for readability, but it is not yet the definitive version of record. This version will undergo additional copyediting, typesetting and review before it is published in its final form, but we are providing this version to give early visibility of the article. Please note that, during the production process, errors may be discovered which could affect the content, and all legal disclaimers that apply to the journal pertain.

Properties of scaffolds prepared by fused deposition modeling of poly(hydroxyalkanoates)

Adriana Kovalcik[1]*, Leire Sangroniz[2], Michal Kalina[3], Katerina Skopalova[4], Petr Humpolíček[4], Maria Omastova[5], Norbert Mundigler[6], Alejandro J. Müller[2,7]**

[1]Department of Food Chemistry and Biotechnology, Faculty of Chemistry, Brno University of Technology, Purkynova 118, 612 00 Brno, Czech Republic

[2]POLYMAT and Polymer Science and Technology Department, Faculty of Chemistry, University of the Basque Country UPV/EHU, Paseo Manuel Lardizabal 3, 20018. Donostia, San Sebastian, Spain

[3]Department of Physical and Applied Chemistry, Faculty of Chemistry, Brno University of Technology, Purkynova 118, 612 00 Brno, Czech Republic

[4]Centre of Polymer Systems, Faculty of Technology, Tomas Bata University in Zlín, třída Tomáše Bati 5678, 760 01 Zlin, Czech Republic

[5]Polymer Institute, Slovak Academy of Sciences, Dubravska Cesta 9, 845 41 Bratislava 45, Slovak Republic

[6]Department of Agrobiotechnology, Institute of Natural Materials Technology, Konrad Lorenz Strasse 20, 3430 Tulln, Austria

[7]IKERBASQUE, Basque Foundation for Science, Bilbao, Spain.

*Corresponding author. Department of Food Science and Biotechnology, Chemical Faculty, Brno University of Technology, Purkynova 118, 612 00 Brno, Czech Republic, kovalcik@fch.vut.cz, adriana.kovalcik@gmail.com (A. Kovalcik)

** Corresponding author. POLYMAT and Polymer Science and Technology Department, Faculty of Chemistry, University of the Basque Country UPV/EHU, Paseo Manuel Lardizabal 3, 20018. Donostia-San Sebastian, Spain and IKERBASQUE, Basque Foundation for Science, Bilbao, Spain, alejandrojesus.muller@ehu.es

 (A.J. Müller).

Abstract
Poly(hydroxyalkanoates) are biodegradable and biocompatible polymers suitable for tissue engineering. Fused deposition modeling (FDM) belongs to modern rapid prototyping techniques for the fabrication of scaffolds. In this work, poly(3-hydroxybutyrate (PHB), poly(3-hydroxybutyrate-co-3-hydroxyvalerate) (PHBV) and poly(3-hydroxybutyrate-co-3-hydroxyhexanoate) (PHBH) were tested for FDM. Thermal and rheological properties of industrial PHAs were compared with poly(lactic acid) (PLA), which is a biodegradable polymer commonly used for FDM. The massive decrease in viscosity and loss of molecular weight of PHB and PHBV precluded their use for FDM. On the other hand, the thermal stability of PHBH was comparable to that of PLA. PHBH scaffolds prepared by FDM exhibited excellent mechanical properties, no cytotoxicity and large proliferation of mouse embryonic fibroblast cells within 96 hours. The hydrolytic degradation of PHBH and PLA scaffolds tested in synthetic gastric juice for 52 days confirmed a faster degradation of PHBH than PLA. The decrease in molecular weight confirmed the first-order kinetics with a slightly higher (0.0169 day^{-1}) degradation rate constant for PHBH as compared to

the value (0.0107 day^{-1}) obtained for PLA. These results indicate that PHBH could be used to produce scaffolds by FDM with application in tissue engineering.

Keywords: Biodegradation, cytocompatibility, mechanical properties, poly(hydroxyalkanoates), poly(lactic acid), 3D printing

1. Introduction

Poly(hydroxyalkanoates) (PHA) are biopolymers synthesized in the form of intracellular granules by a wide range of microorganisms as carbon and energy storage materials. Recently, PHAs have attracted large attention because they meet several criteria as biomaterials and also for their potential use in drug delivery and tissue engineering [1, 2]. Tissue engineering is a new interdisciplinary and multidisciplinary field that belongs to the area of biomolecular engineering, where, despite great progress, many different challenges remain [3]. The basic aims of tissue engineering are the understanding of the structure-function relationships in normal and pathological tissues and the development of functional replacements and treatment/regeneration of different tissues and organs. Principally, the damaged tissues are combined with scaffolds, which act as templates for tissue regeneration [4]. Different materials are used for scaffolds production including metals, ceramic biomaterials, polymeric biomaterials, bioactive ceramics and glasses, and polymer/ceramic or polymer/glass composites [5-7]. Materials for scaffolds production should fulfill some criteria according to their application, such as biocompatibility, non-inflammability and often biodegradability. For example, bone regeneration, using tissue engineering, often requires scaffolds with high porosity and tunable bioactivity such as good cell adhesion, proliferation and differentiation [8-10].

PHAs are biocompatible and biodegradable thermoplastics with good mechanical properties and tunable morphology that can be considered biomaterials suitable for tissue engineering applications [1, 11, 12]. PHAs are polyesters with a different chemical nature and a wide range of physical properties. This group of biopolymers comprises homopolymers composed of short-chain-length monomers (scl-PHA, 2 - 5 carbon atoms, stiff and brittle behavior), homopolymers composed of medium-chain-length monomers (mcl-PHA, $\geq$ 6 carbon atoms, elastomeric behavior), and copolymers or terpolymers containing heteromonomers (e.g., 3-hydroxyvalerate, 4-hydroxybutyrate, 3-hydroxyhexanoate). Chemical structure, molecular architecture and physical properties of microbial PHAs depend on the biotechnological production strategy [11, 13, 14]. Different technologies are used to produce PHA scaffolds. Most of those technologies are based on the dissolution of the polymer in toxic solvents such as salt leaching (chloroform) [15], thermally induced phase separation (chloroform and 1,4-dioxane) [16-18], solution casting (chloroform, dichloromethane) [19-21], electrospinning (chloroform, dichloromethane, N,N-dimethyl formamide, 1,1,1,3,3,3-hexafluoro-2-propanol) [22-24], gas-in-oil-in-water double emulsion with CO_2 (methylene chloride) [25], and wet 3D spinning (chloroform) [26]. Recently, considerable solvent-free techniques have attracted great interest, like thermoforming, extrusion, injection molding [27, 28], selective laser sintering [29-32] and fused deposition modeling (FDM) [33]. Selective laser sintering (SLS) and FDM belong to 3D printing technologies; these techniques can produce 3D objects directly according to the individual digital designs. The principle of FDM is polymer extrusion and that of SLS is polymer powder bed fusion. Both methods can process thermoplastics and have advantages and disadvantages [34]. PHAs should be processable by both methods, but PHAs processing using FDM is a challenge. However, there is the problem that PHAs (mainly poly(3-hydroxybutyrate) (PHB)) possess low thermal stability during melt processing and are

degraded quickly [35]. The drop in the molecular weight can be so drastic that the final mechanical properties often do not fulfill the theoretical expectations. The most important challenges are the improvement of PHAs thermal processing window and their practical applications. In order to improve the melt stability of PHAs, different strategies are used, including the incorporation of stabilizers, fillers, crosslinking additives, and anti-hydrolysis agents or blending with other polymers. However, the reduction in molecular weight may still occur and this reduction will depend on the processing conditions.

This study aimed to assess the thermal properties and thermal stability of commercial PHAs and their suitability for the processing of scaffolds by fused deposition modeling. FDM belongs to the group of 3D printing technologies, which enable the production of complex customized products with applications in medicine and pharmacy (implants, scaffolds for tissue engineering, diagnostic platforms, and drug delivery systems) [6]. The basis of FDM is the fusion of thermoplastic filaments and the deposition of molten material in a particular laydown pattern within a few minutes or hours [36]. The FDM process itself is proceeded by the preparation of polymer filaments of a given diameter (usually 1.75 mm) by extrusion. Thermoplastic polymer processed by extrusion should have adequate viscosity values and thermal stability. Among the conventional thermoplastics used for the production of filaments for FDM, the following polymers can be found: acrylonitrile butadiene styrene (ABS), polyethylene terephthalate (PET), poly(lactic acid) (PLA), thermoplastic elastomer (TPE), thermoplastic copolyester (TPC) and composites made of the polymers mentioned above reinforced with various fillers. Actually, filaments based on PLA and PHA blends are commercially available [37-39]. However, the type and concentration of the PHA employed in PLA/PHA filaments is unknown. Among the most investigated PHA, mostly poly(3-hydroxy butyrate) (PHB) can be found. PHB is a semi-crystalline polyester with a high degree of crystallinity, high brittleness and low thermal stability during melt processing [40]. The incorporation of PHB to PLA accelerates the crystallization and improves the processability of PLA by polymer processing methods such as injection molding and FDM [41]. The blending of PLA with PHB is favorable and results in a material with better rheological, barrier and mechanical properties compared to neat PLA or PHB [40, 42]. In addition to PHB, other types of PHA are also blended with PLA to improve the impact properties of the material, but often the chemical structure of PHA is unknown or cannot be published due to the limitations given by the polymer producer [43]. This research focuses on 1) investigation and comparison of thermal and rheological properties of different commercial PHAs, 2) evaluation of their suitability for FDM and 3) processing of scaffolds by FDM and assessment of their thermal properties, mechanical properties, cytotoxicity, and degradation in synthetic gastric juice. Since PLA belongs to the commonly used thermoplastic for FDM, the properties of PHA scaffolds were compared with PLA scaffolds.

2. Experimental part

2.1. Materials

Poly(lactic acid) (PLA 2003D) with a D-isomer content of 4 %, a density of 1.24 g cm^{-3}was purchased from NatureWorks, Minnetonka, MN, USA. Poly(hydroxybutyrate-co-hydroxyhexanoate) (PHBH X131A) with a density of 1.2 g cm^{-3} was purchased from Kanaeka Corporation, KITA-KU Osaka, Japan. Poly(hydroxybutyrate) (PHB Hydal) with a density of 1.1 g cm^{-3} was provided by Nafigate Corporation, Prague, Czechia. Poly(hydroxybutyrate-co-hydroxyvalerate) (PHBV, Mirel P1004) with a density of 1.3 g cm^{-3} was purchased from Telles Inc., USA. Table 1 shows molecular weight properties (M_n number–

average and M_w weight–average), polydispersity (Đ) and melt volume rates of polymers determined in this study. These data were determined within this study.

Filaments with a thickness between 1.6 – 1.75 mm were prepared by extrusion with previously dried polymers by FilaFab PRO 350 extruder (FD3D Innovations Limited, UK) at 150 °C (PHBH) and 185 °C (PLA) at 20 rpm. The scaffolds were printed with 3D printer Original Prusa I 3MK3S (Prusa Research, Czechia) at a nozzle temperature of 205 °C and a printing bed temperature set to 60 °C. For cytotoxicity tests, thermal properties and degradation in digestive fluid rectangular scaffolds of 35 ×21 × 0.34 mm were printed. For tensile testing and dynamic mechanical analysis, dumb-bell shaped specimens were printed.

2.2. Characterization methods

2.2.1 Polarized light optical microscopy (PLOM)

A polarized light optical microscope, Olympus BX51 equipped with an Olympus SC50 digital camera and with a Mettler Toledo FP82 hot stage, was employed to determine the crystalline morphology of biopolymers. The samples were prepared by solution casting employing chloroform as a solvent, obtaining films with a thickness of about 50 μm. Those films were sandwiched between two glass slides to analyze them by PLOM. Samples were first heated to 190 °C to erase their thermal history and then cooled down to 70 °C. The heating and cooling rates employed were 20 °C min^{-1}.

2.2.2 Differential scanning calorimetry

DSC experiments were performed using a DSC 8000 (Perkin Elmer) under a nitrogen atmosphere. The calibration of DSC was accomplished with high purity indium. Samples of about 10 mg were hermetically sealed in aluminum pans. The samples were tested employing non-isothermal and isothermal experimental protocols.

Non-isothermal DSC experiment was carried out heating the sample from 25 °C to 190 °C, cooling from 190 °C (165 °C in case of PHBH) to -20 °C and heating again from -20°C to 190 °C with heating/cooling rates of 20 °C min^{-1}.

The isothermal crystallization kinetics of PHAs were determined according to the protocol developed by Lorenzo et al. in which the minimum isothermal crystallization temperature is first determined by trial and error (see more details in Ref. [44]). This temperature represents the starting point to perform the isothermal experiments displayed in Table 2.

2.2.3 Thermal, rheological and mechanical properties

Thermogravimetric analysis (TGA) was performed by TGA Q50 (TA Instruments, USA) with an airflow of 60 mL min^{-1}. Approximately 5 mg of the sample was sealed in an aluminum crucible and was heated from 25 °C to 500 °C with a heating rate of 10 °C min^{-1}.

Melt volume rate (MVR) of polymers was determined according to ISO 1133 (190°C, 2.16 kg) using an Instron Ceast ISO MF20 melt flow tester.

The rheological characterization of PLA and PHA samples was performed employing an ARG-2 rheometer (TA Instruments, USA) with a 25 mm parallel-plate geometry. Frequency sweeps were performed in the linear viscoelastic regime from 628.3 to 0.16 rad s^{-1}. In order to analyze the thermal degradation of the samples during extrusion, time sweeps were carried out at 1 Hz for 40 minutes at the adequate temperature for each sample.

Mechanical properties of the extruded filaments and the FDM processed dumb-bell shape specimens (with the same structure as scaffolds) were measured on an Instron 3365 (Instron, USA). The gauge length was 20 mm and the thickness of the samples was 0.34 mm. The applied strain rate was 1 mm min $^{-1}$. Average values of Young's modulus (E), tensile stress at maximum (σ_B) and tensile strain at break (ε_B) were calculated from stress/strain plots of five specimens.

Dynamic mechanical analysis (DMA) was carried out in a dynamic oscillatory mode using a DMA Q800 (TA Instruments, USA). Strips with a width of 4 mm were cut from the dumb-bell shape specimens with a gauge length of 7 mm and a thickness of 0.34 mm. Viscoelastic properties such as storage modulus (E') and mechanical loss factor (tan δ = loss modulus/storage modulus) were determined at atmospheric air by applying dynamic oscillatory measurement using a frequency/strain experimental setup with the following conditions: isotherm at -60 °C for 10 min, heating up to 120 °C at a rate of 3 °C min^{-1} and oscillation of 1 Hz.

2.2.4 Cytocompatibility

Two experiments have been performed to reveal the cytocompatibility of scaffolds. Firstly, the cytotoxicity of extracts from scaffolds was tested to analyze the fundamental biological properties of the scaffolds. Subsequently, the proliferation of cells seeded on the scaffolds was determined. The cytotoxicity was determined using a mouse embryonic fibroblast cell line (ATCC CRL-1658 NIH/3T3, USA). ATCC-formulated Dulbecco's Modified Eagle's Medium (PAA Laboratories GmbH, Austria) containing 10% bovine calf serum (BioSera, France) and 100 U mL^{-1} of Penicillin/Streptomycin (GE Healthcare HyClone, United Kingdom) was used as the cultivation medium. The cytotoxicity test was performed according to the ISO standard 10992-12. Extraction was performed in chemically inert closed containers using aseptic techniques at 37 °C under stirring for 24 h. On day one, sample extracts were prepared and cells were seeded to pre-incubate in the microtitration test plates with a concentration of 1×10^5 cells per mL. The cells were incubated at 37 °C in 5 % CO_2 in humidified air for 24 hours. On the second day, the extracts were diluted with culture medium to obtain the following concentrations: 100, 50, 25, and 10 % of parent extract. All assays were performed in quadruplets. The medium was sucked from plates and replaced by individual extracts. The plates with extract were incubated for 24 hours. Cell viability was determined by using 3-(4,5-dimethylthiazol-2-yl)-diphenyltetrazolium (MTT cell proliferation assay kit, Duchefa Biochemie, Netherlands) assay. The absorbance was measured at 570 nm and the reference wavelength was fixed on 690 nm. The results are presented as the reduction of cell viability in percentage when compared to cells cultivated in medium without the extracts of the tested materials. The results of the cell viability were studied from the point of view of statistical significance by the analysis of variance employing Origin (version Origin Pro 2018). Differences among mean values were processed by the Tukey test at a level of significance of $p < 0.05$. The morphology of the cells from the culture plates was observed using an inverted Olympus phase-contrast microscope (IX 81).

In the proliferation tests, mouse embryonic fibroblast cell lines (ATCC CRL-1658 NIH/3T3, USA) were used. Before testing the proliferation, the polymer scaffolds have been sterilized by exposition to UV light for 30 min. Two sets of samples have been prepared: set A with non-treated scaffolds and set B with scaffolds coated with 0.1 % solution of gelatine. The samples were cultured in a cell suspension at an initial concentration of 1.10^5 cells mL^{-1}. After 90 minutes of the cells adhering, the cell suspension was sucked and a new culture medium was added. After 96 hours (4 days) of proliferation, the cells were fixed and stained with Hoechst 33258 (Molecular Probes, Carlsbad, CA) and ActinRed 555 (Life

Technologies, USA). Cells were incubated at 37°C in 5% CO_2 in humidified air. As reference cells attached to the tissue culture plate was used. The morphology of the cells has been investigated using a confocal microscope (Olympus).

2.2.5 Degradation of scaffolds in model digestive fluid and determination of molecular weight

The degradation rate of the scaffolds (35 × 21 × 0.34 mm) was studied by their incubation (duration 52 days) at 37 °C in synthetic gastric juice prepared according to Atkins and Peacock (pH 1.6, pepsin 0.7 U mg^{-1}) [45]. The progress of process was monitored by periodic measurement of residual mass weight, average molecular weight (M_n and M_w) and the polydispersity of the scaffolds in time.

2.2.6 Molecular weight and polydispersity determination

Molecular weight (M_n number–average and M_w weight–average) and polydispersity (Đ = M_w/ M_n) of the source polymers (PLA, PHB, PHBH, PHBV) as well as the scaffolds obtained from degradation study in model digestive fluid was measured by size exclusion chromatography (SEC Infinity 1260 system, size separation by PL gel MIXED-C column, Agilent Technologies, USA) coupled with Dawn Heleos II multiangle light scattering (MALS) detector (Wyatt Technology, USA) and Optilab T-eEX differential refractometer (dRI, Wyatt Technology, USA). The individual samples were dissolved in chloroform (4 mg mL^{-1}) for 3 hours at 70 °C and filtered before analyses (0.45 µm syringe filter with nylon membrane). Chloroform was used as eluent at a flow rate of 0.6 ml min^{-1}, the measurement temperature was 25 °C and the sample injection volume was 100 µL. For each analyzed sample the measurement was performed in three replicates. The obtained molecular weights were calculated by ASTRA software (Wyatt Technology, version 6.1) using the value of the refractive index increment of PHB and PHBV (dn/dc = 0.0336 mL g^{-1}), PHBH (dn/dc = 0.0462 mL g^{-1}) and PLA (dn/dc = 0.0265 mL g^{-1}). These values of dn/dc were determined by the batch measurement of the concentration dependence of the absolute refractive index of individual polymers (concentration in the range from 3.6 to 5.6 mg/mL) using Optilab T-eEX differential refractometer (dRI, Wyatt Technology, USA) equipped with syringe pump with adjustable flow-rate and a manual injection valve (Model R99-E, Razel Scientific).

3. Results and discussion
Thermal properties of polymers
Non-isothermal crystallization

The thermal behavior of PLA and PHA polymers were studied by non-isothermal and isothermal DSC experiments. The data of non-isothermal DSC are summarized in Table 3. Figure 1 shows the DSC cooling and second heating scans. The PLA employed in this work cannot crystallize or melt at 20 °C min^{-1}. This indicates that the D-content of 4 % slows down the crystallization rate and if the material is cooled at a rate as fast as 20 C min^{-1} it remains completely amorphous [46]. The crystallization was so slow that even at a cooling rate of 2°C min^{-1} the material could not crystallize [47]. The advantage of the amorphous structure is that the materials have low shrinkage.

In contrast to PLA, all investigated PHAs are semi-crystalline polyesters (Table 3). The crystallization behavior of PHA polymers depends on their chemical composition, the presence of additives (e.g., nucleating additives) and processing conditions. PHB crystallizes very slowly, as it exhibits a very small crystallization peak during cooling (see Figure 1a) and a cold crystallization peak during the heating scan (Figure 1b). This polymer shows the lowest crystallization temperature, 41.1 °C, followed by PHBH, which has a T_c of 82.9 °C, and finally, the sample with the highest T_c is PHBV, with a value of 101.9 °C. PLOM micrographs indicate that PHBH and PHBV have a much higher number of nuclei (producing much smaller spherulites) and this can explain their higher crystallization temperatures, as the non-isothermal

crystallization temperature, when a polymer is cooled from the melt, is a function of the nucleation density.

Figure 1b shows some complex bimodal melting for PHBV and PHBH, which merits an in-depth study to ascertain its origin, but that is outside the scope of the present work. This bimodal melting could be due to reorganization during the scan or the presence of two different polymorphs. In general, one would expect a reduction in melting point and crystallinity when PBH is randomly copolymerized with hydroxyvalerate or hydroxyhexanoate depending on the amount of comonomer incorporated. If the melting enthalpy of the second heating scan is analyzed, see Table 3, it can be observed that PHB has the highest melting enthalpy, whereas PHBH and PHBV show a significantly lower melting enthalpy. One would need to determine the copolymers composition to be able to normalize the melting enthalpies by PHB content to quantitatively determine the reduction in crystallinity that could be present in the copolymers, in comparison with PHB homopolymer. The melting point of PHBH is lower than that of PHB as expected; however, that of PHBV is higher for unknown reasons.

Figure 2 shows polarized light optical micrographs of biopolymers cooled from the melt at a constant rate of 20 °C min^{-1}. Spherulites are observed in all PHA samples except PLA, which is amorphous. PHB exhibits very large spherulites with a diameter larger than 100 micrometers. It is well known that PHB has very low nucleation rates, hence it can form very large spherulites (as the growth rate is much larger than the nucleation rate) [48]. The formation of large spherulites induces stress concentration around the interspherulitic regions leading to low impact resistance and brittleness [49].

On the other hand, PHBH and PHBV contain a large number of small spherulites. Copolymerization can induce nucleation enhancement in random copolymers [50]. Additionally, both copolymers are obtained industrially and they may contain nucleating agents.

Overall Isothermal crystallization behavior

The results of the isothermal crystallization are listed in Table 4 below. The experimental data obtained by isothermal crystallization was fitted to Avrami equation [51]:

$$1 - V_c(t - t_0) = \exp(-k(t - t_0)^n) \qquad (1)$$

where V_c is the relative volumetric transformed fraction, k is the overall crystallization rate constant and n is the Avrami index.

Table 4 shows the values of Avrami fitting parameters. The Avrami index reflects the geometry of the crystalline structures and the kinetics of the nucleation process. If spherulitic structures are formed, i.e., 3-dimensional structures, the Avrami index should be between 3 and 4. On the contrary, if axialites are constituted, 2-dimensional structures, the Avrami index takes a value between 2 and 3. If the nucleation is instantaneous when spherulites are formed, the Avrami index takes a value of 3, whereas if it is sporadic, the Avrami index should be 4. In the case of axialites, when the nucleation is instantaneous, the Avrami index is equal to 2, whereas if it is sporadic, it will take a value of 3.

The values of the Avrami index obtained for PHB and PHBV were generally in a range of values that can be approximated to 2-4 and 3-4, respectively, as can be seen in Table 4. The increase of the Avrami index with the higher crystallization temperature indicates that the morphology of crystals changes from axialites to spherulites as could be expected, since at higher T$_c$, i.e., lower supercooling, each spherulite can grow with less restriction (i.e., impingement with the neighboring spherulites does not occur in the

initial stages of the crystallization process) forming 3-dimensional structures. At low supercoolings also sporadic nucleation occurs, which results in Avrami index values near 4. Regarding the overall crystallization rate constant, as could be expected, it is reduced by increasing the crystallization temperature.

One important result that can be appreciated in Table 4 for PHB, as well as for PHBV, is that the melting temperature values measured after the isothermal crystallization do not increase with T_c. This means that most probably, degradation occurred during the isothermal measurements. This is one of the problems associated with both PHB and PHBV, as they tend to degrade as soon as they are melted. The results reported in Table 4 are, therefore, influenced by degradation and cannot be used to extrapolate equilibrium melting temperatures.

On the other hand, the results of Table 4 exhibit the expected trends for PHBH, as its melting point increases with T_c values. In fact, Figure 3 shows that the determination of the equilibrium melting temperature was possible by employing the Hoffman-Weeks extrapolation. A reasonable value of 156.5 ºC was obtained, which is approximately 13 ºC higher than the highest experimental melting point obtained at high T_c values. This value is comparable with the value determined by Xu et al. (T_m^0 of PHBH = 159.4 °C) [44]. The equilibrium melting temperature of poly(hydroxyalkanoates) markedly depend on their chemical structure, copolymer composition and molecular weight [52, 53].

Regarding PHBH, most Avrami index values were in a range close to 3.5, being the variation of the index very subtle. In this case, a spherulitic structure is most likely obtained with a nucleation process that becomes more sporadic increasing the T_c since the Avrami index increases. In fact, the PLOM of Figure 2 shows very small but recognizable spherulites for PHBH after non-isothermal crystallization. The theoretical half crystallization times are in full agreement with the experimental half crystallization times, which shows that the Avrami equation can predict the overall isothermal crystallization, fitting very well the experimental values.

The results of the isothermal crystallization experiments indicate that PHBH does not seem to experience thermal degradation, at least within the level that can be detected by DSC (especially considering the changes in T_m values with T_c).

Thermal stability

TGA was used to assess the thermal stability of polymers in air. Figure 4 shows the TGA curves of PHB, PHBV, PHBH and PLA up to 500 °C. The onset of thermal degradation, the temperature with the maximum sample weight-loss and the residual mass at 500 °C obtained from TGA curves are reported in Table 5. The values of the onset of thermal degradation (T_{onset}) show that PLA is the most stable material since it has the highest T_{onset}, 282 °C. PLA is followed by PHBH and PHB, which shows an onset of thermal degradation temperature of 250.9 °C and 243.1 °C. The material with lower thermal stability is PHBV since its thermal degradation begins at 230.1 °C, which is 51.9 °C lower than the onset degradation temperature of PLA. Similarly, the values of the temperatures at the maximum weight-loss rate (T_{max}), indicate that PLA is more stable than the analyzed PHAs. PHBV and PHBH are copolymers and exhibit two main maximum weight-loss rate peaks. The values at the maximum weight-loss rate depend on the molecular weight of polymers and the presence of fillers or other additives. The values of the onset of thermal degradation (T_{onset}) show that PLA is the most stable material since it has the highest T_{onset}. The temperature with the maximum weight loss rate of PHBV is comparable with that of PLA although PHBV

8

starts to degrade at lower temperatures. PHBV is the only material that shows a residue at 500 °C, this residue of 2.8 % indicates the presence of a very stable additive. The presence of this additive may explain why the temperature at the maximum weight loss of PHBV is comparable with that of PLA. From the point of view of melt processing, the most indicative parameter is the onset of thermal degradation; according to this parameter, the thermal stability follows this order from the most stable to the least stable material: PLA > PHBH > PHB > PHBV.

In order to predict the behavior of polymers during melt processing such as extrusion and FDM, rheological measurements were performed. It is known that the viscoelastic and mechanical properties of products based on biodegradable polyesters depend on the applied processing conditions (humidity, processing temperature, shear stress and time) and on the presence of additives [35, 54]. The rheological behavior of PHAs and PLA was determined at a temperature well above the melting peak (considering the first scan obtained by DSC), ensuring the complete melting of the sample. The same temperature was used for the extrusion of filaments.

Figure 5 shows the behavior of the complex viscosity as a function of frequency. Considering the behavior of the polymers, the materials could be divided into two groups; the first group is constituted by PLA and PHBV, those polymers show a significant Newtonian behavior over a wide frequency range. A slight reduction of the viscosity, i.e., pseudoplasticity, is observed at frequencies above 20 rad s^{-1}. PHBV shows a slight increase of the viscosity at low frequencies, which could result from the presence of the additive, which is able to form a percolated network, which results in a slight pseudoplastic behavior. If the viscosity values are compared, PHBV shows very low viscosity values, about 51 Pa s, therefore its melt processing without the addition of efficient stabilizers is excluded. In order to process the polymers by extrusion to obtain the filament or to perform FDM, the materials require some melt strength, with an adequate viscosity value. The viscosity of PHBV is very low, so it does not have adequate melt strength. Regarding the second polymer group, constituted by PHB and PHBH, they show a significant pseudoplastic behavior, which indicates that these materials are sensitive to processing conditions such as shear and frequency. PHBH shows the highest viscosity, almost 2 order of magnitudes higher than PLA at low frequencies. Regarding PHB, it shows a viscosity value about one order of magnitude higher than PLA at low frequencies.

The susceptibility of PHAs to thermal degradation was further studied by carrying out three frequency scans in total, employing the same sample. Table 6 shows the values of the Newtonian viscosities determined from the three frequency sweep measurements, according to the following equation:

$$\eta' = \frac{\eta_0}{1+(\omega\lambda_0)^\alpha} \qquad (2)$$

where η_0 is the Newtonian viscosity, λ_0 the relaxation time and α a non-linearity index.

The reduction of the viscosity of PLA, PHB, PHBV and PHBH after three frequency sweep runs were 3.3 %, 26.6 %, 22.9 % and 7.3 %, respectively. Therefore, the most stable materials, i.e., the polymers with the lowest viscosity reduction, were PLA and PHBH. The reduction of viscosity results from the decrease of the molecular weight due to thermal degradation.

The reduction of viscosity was further studied by normalizing the initial complex viscosity values at t = 0 min over time (see Figure 6). PHB and PHBV displayed a significant reduction of the viscosity for 40 minutes. The recorded decrease in viscosity indicates that the processing of filaments from PHB and PHBV via the extrusion process will not be possible due to the drastic thermal degradation during melt processing. Regarding PHBH, in this case, there is only a slight viscosity reduction similar to that of PLA. Therefore, thermal processing and preparation of the filaments from PHBH should be possible without a severe change in molecular weight.

Mechanical and viscoelastic properties of filaments and scaffolds

Considering the thermal stability of the poly(hydroxyalkanoates) studied in this work, the most suitable material for the preparation of filaments and scaffolds is PHBH. Thus, filaments for FDM made from PHBH have been prepared. With the PHBH filaments, the scaffolds have been prepared and the properties of those PHBH scaffolds have been compared with PLA scaffolds (see Figure 7).

Table 7 summarizes the mechanical properties of filaments and scaffolds made from PHB and PLA. The scaffolds exhibited about 125 % (PLA) and 269 % (PHBH) higher elastic modulus than the original filaments. The values of the tensile strength and elongation at break of scaffolds are much lower than the original filaments. These changes correspond to the processing history and the geometry of the samples. A very important factor in polymer melt processing is the thermal stability of the polymer. Although it has not been tested and was not among the aims of the present study, the thermal stability and mechanical performance of PHAs could be improved by the addition of inorganic nanofillers such as silver nanoparticles, zinc oxide nanoparticles, graphene oxide (GO) or molybdenum disulfide nanosheets embedded with nanodiamond particles [55-58]. Recent studies showed that the incorporation of co-dispersed nanostructures support the better distribution of nanofillers in the polymer matrix and certain combinations of nanofillers may involve even a synergistic effect on improving the mechanical behavior and antibacterial activity of the scaffolds [58, 59].

Mechanical properties of PHBH filaments and scaffolds are lower compared to those of PLA, but it corresponds with their semi-crystalline state and viscoelastic behavior at room temperature. The stiffness of scaffolds measured at room temperature reflects the fact that PLA is amorphous and glassy at room temperature; hence, it has a high elastic modulus, as expected. On the other hand, PHBH is a semi-crystalline polymer with a lower elastic modulus, as at room temperature it is between T_g and T_m.

DMA measurements were carried out to analyze the behavior of the viscoelastic properties of PHBH and PLA scaffolds in the temperature range from -20 °C to 105 °C. The temperature-dependent curves of storage moduli and loss factors of PLA and PHBH scaffolds are presented in Figure 8. Storage moduli characterize the ability of the scaffolds to store energy and reflect their stiffness.
As shown in Figure 8, PHBH scaffolds have about 47 % higher storage modulus than PLA scaffolds at temperatures below 0°C. The values of the storage moduli of both materials decreased with increasing temperature, as expected (Table 8). When the temperature reaches the T_g of each material, i.e., the temperature corresponding to the maximum of tan δ or the inflection point of the elastic modulus, the elastic modulus drops markedly. In the case of PLA, above the T_g the material shows the typical rubbery behaviour with a very low storage modulus (as it is an amorphous material), however, PHBH shows a more gradual reduction of the storage modulus so, the material keeps some rigidity even above the T_g, as expected for a semicrystalline material below T_m. As shown in Figure 8, the values of loss factors

confirmed the different crystalline character of PLA and PHBH scaffolds. The tan δ peak of PLA scaffolds reaches a value of about 1.8. This high value indicates an amorphous character of the sample. In comparison, the tan δ peak of PHBH scaffolds reached a value of 0.1, which indicates a high degree of crystallinity since the presence of crystals hinders the mobility of polymer chains in the amorphous regions of the sample, which results in lower tan δ values.

Cytocompatibility

The cytocompatibility of any biomaterial is crucial for its applicability. The absence of cytotoxicity must be considered as an essential property in tissue engineering. In the present study, the cytotoxicity of the extracts of PLA and PHBH scaffolds have been tested by MTT assay. Figure 9 shows the quantitative analyses of cytotoxicity of extracts of scaffolds in followed dilution with cultivation media: 10 %, 25 %, 50 % and 100 %. All extracts received relative values of viability higher than 0.8, which means they do not induce any cytotoxic effect. Moreover, the statistical analysis, ANOVA, showed that all groups of extracts are considered to have equal variance and do not show significant differences.

As all the prepared scaffolds do not induce the cytotoxic effect, the test of cell adhesion and proliferation was performed on all samples. The experiment was conducted in two sets, the adhesion and proliferation on A) pure scaffolds without additional surface treatment or on B) the surface of scaffolds which were covered by gelatine, which is commonly used material improving the initial adhesion of cells on the surfaces. The results are shown in Figure 10. It is clearly seen that compare to reference (Tissue Culture Plastic), the cells do not adhere and proliferate well on the PLA scaffolds. The cytocompatibility was not significantly improved even by coating with gelatine. The PHBH scaffolds demonstrate also very good cytocompatibility.

As shown in Figure 10D and 10E, the number and morphology of cells were sufficiently comparable to reference in the case of pure PHBH as well as PHBH coated with gelatine. The results obtained correlate with the study by Yang et al. Their experiments have shown that PHBH promotes cell growth compared to PLA. Proliferation was evaluated using murine fibroblasts L929. After lipase treatment, the cells on the samples were able to proliferate even better [60]. Similar findings were achieved in the work of Shangguan et al., PHBH and PLA films were tested in this study. The proliferation of cells on PHBH was higher than on PLA films. In this study, the PHBH material was physically modified to improve cell growth. However, it was not the resultant film that was modified by UV radiation, but the powder used for their production [61]. Another possible surface modification of the PHA scaffolds is coating by silk fibroin. Silk fibroin encourages cell adhesion without altering the mechanical properties of the material [62]. Other researchers indicated that the biocompatibility of polymer scaffolds could be enhanced by the admixing of superparamagnetic Fe_3O_4 nanoparticles [57, 63]. Shuai et al. presented that the action of the magnetic field provided a more favorable physicochemical and biological microenvironment for cell adhesion, growth, proliferation and differentiation of polyglycolic acid/Fe_3O_4 scaffolds [63].

As already mentioned, in this work the surface was modified by coating it with 0.1 % gelatine. However, proliferation was almost identical if the treated and untreated samples are compared. Gelatine mainly promotes the initial adhesion of the cells. The proliferation of NIH/3T3 cells on PHBH scaffolds was much better than on PLA scaffolds (see Figure 10). This shows that the materials prepared in this work can be applied even without further surface modification.

Abiotic degradation of scaffolds in model digestive fluid

The degradation of PLA and PHBH scaffolds in synthetic gastric juice (*in vitro*, pH = 1.6, 37 °C) has been monitored for 52 days. Both PLA and PHBH are polyesters that are sensitive to hydrolysis. The key parameters that influence the degradation rate of aliphatic polyesters in fluids include chemical structure, molecular weight and distribution, sample geometry and morphology (thickness, porosity), processing history (crystallinity) and hydrolysis conditions [64]. The results of the mass weight and molecular weight changes obtained during the degradation of PLA and PHA scaffolds are displayed in Table 9.

During the first twenty days, the values of the mass weight of both types of scaffolds increased slightly, being this increase more pronounced for PLA. It should be considered that PLA is almost completely amorphous and that the water absorption of the amorphous region is higher in comparison with the crystalline regions.

A better way of analyzing the evolution of abiotic degradation of polyesters is to study the variation of molecular weight during time. The carboxylic esters bearing a tertiary beta-hydrogen start to decompose and the molecular weight of polymer decreases, while non-degraded polymer chains start to reorganize and crystallize (see Figure 11 and Table 10). Prior to degradation, the PLA scaffold had a specific melting enthalpy $\sum\Delta H$ = 2.9 J g^{-1}, hence a very small crystallinity degree of X_c = 3.1 %. After 52 days of abiotic degradation, the enthalpy increased to 27.2 J g^{-1} (X_c = 29.2 %). This indicates that degradation occurs during this period, as will be mentioned later, the molecular weight is reduced, which promotes the crystallization. However, in the case of PHBH, the degree of crystallinity of PHBH after 52 days of abiotic degradation increased only slightly. The similar melting enthalpy value can be explained considering that prior to degradation, PHBH could be near the maximum crystallization degree of the material.

In the second step of degradation (after 40 days), scaffolds started to lose their mass due to the deterioration of crystalline regions and were very brittle. The most relevant parameter to check if degradation occurs is the molecular weight of residual polymers. As can be seen in Table 9, during the abiotic degradation of the samples, there is a progressive reduction of the molecular weight for both studied polymers. The reduction of the molecular weight of the scaffolds after 52 days of incubation in synthetic gastric juice reached about 43.6 % for PLA scaffolds and 62.7 % for PHBH scaffolds. As was already described in the literature [65, 66], the hydrolytic degradation of PLA and PHB-based copolymers is dependent on many factors including polymer chain length, crystallinity, molecular weight distribution, surface pretreatment, porosity and processing conditions, but in summary the rate of the process can be described using a first order kinetics, according to:

$$M_{w(t)} = M_{w(0)} \cdot \exp(-k_D\tau) \qquad (3)$$

where $M_{w(0)}$ is the molecular weight at the beginning of the experiment, k_D is a degradation rate constant of the first order kinetic of degradation and τ is the duration scaffold degradation in gastric juice.

The observed decrease of molecular weight in time for both studied scaffolds showed typical exponential decay, which confirmed the adequacy of using a first order kinetics for modeling polymer degradation in our study (see in linearized form in Fig. 12).

The application of the kinetic model provided the value of k_D = (0.0107 ± 0.0007) day^{-1} for PLA and slightly higher value of k_D = (0.0169 ± 0.0030) day^{-1} for PHBH. These rate constants of degradation represent important parameters for further modeling and prediction of changes in molecular weight in time and for theoretical calculation of actual molecular weight of the polymer in the scaffold. The result

also indicates that degradation is faster in the case of PHBH scaffolds than in PLA, which could be advantageous for some biomedical applications. Our data are also in good agreement with the values published in the literature [52], where the authors used first order kinetics for degradation modeling of PLA, PHA and other polysaccharides hydrolysis in aqueous buffers. They obtained a value of $k_D = 0.0117$ day^{-1} for PLA and observed a faster rate of degradation for PHA-based polymers and copolymers in comparison with PLA, which confirms our results.

Conclusions

In this work, the suitability of different poly(hydroxyalkanoate)s with potential applications in biomedicine have been studied. Among the different PHAs studied, it has been found that poly(hydroxybutyrate-co-hydroxyhexanoate) has adequate thermal stability and rheological properties to be used in FDM. The assessment of PHB and PHBV thermal degradation showed that these polymers are susceptible and markedly degrade during repeating melt processing. The rheological and mechanical properties of the filaments prepared from PHBH confirmed that they are sufficient for fused deposition modeling.

Scaffolds prepared from PHBH by FDM have shown good mechanical and viscoelastic properties. These scaffolds showed no cytotoxicity. The cytocompatibility in terms of cell proliferation showed significant differences as PLA scaffolds do not allow the cells to proliferate on their surfaces, while the PHBH scaffold surface allowed the cell proliferation comparable to tissue culture plastic. Compared to PLA scaffolds, PHBH promoted much higher cell proliferation and faster abiotic degradation in model digestive fluid. It can be concluded that PHBH possesses excellent properties to be used as material for scaffolds. These results illustrate that PHBH could expand the offer of biodegradable polymers used for fused deposition modeling, offering excellent biocompatibility and biodegradability in body fluids.

Acknowledgments

Conflicts of Interest
The authors declare no conflict of interest.

References

[1] J. Lim, M. You, J. Li, Z. Li, Emerging bone tissue engineering via Polyhydroxyalkanoate (PHA)-based

scaffolds, Mat. Sci. Eng. C 79 (2017) 917-929.

[2] E. Elmowafy, A. Abdal-Hay, A. Skouras, M. Tiboni, L. Casettari, V. Guarino, Polyhydroxyalkanoate

(PHA): applications in drug delivery and tissue engineering, Expert Rev. Med. Devic. 16(6) (2019) 467-

482.

[3] P.X. Ma, Scaffolds for tissue fabrication, Mater. Today 7(5) (2004) 30-40.

[4] F.J. O'Brien, Biomaterials & scaffolds for tissue engineering, Mater. Today 14(3) (2011) 88-95.

[5] W.M. Saltzman, Biomedical Engineering: Bridging Medicine and Technology, Cambridge University Press, Cambridge, 2009.

[6] H.N. Chia, B.M. Wu, Recent advances in 3D printing of biomaterials, J. Biol. Eng. 9(1) (2015) 4.

[7] A.R. Boccaccini, J. Gough, Tissue Engineering Using Ceramics and Polymers, Woodhead Publishing Limited, Abington Hall, England, 2007.

[8] C. Gao, S. Peng, P. Feng, C. Shuai, Bone biomaterials and interactions with stem cells, Bone res. 5(1) (2017) 1-33.

[9] P. Feng, P. Wu, C. Gao, Y. Yang, W. Guo, W. Yang, C. Shuai, A multimaterial scaffold with tunable properties: toward bone tissue repair, Adv. Sci. 5(6) (2018) 1700817.

[10] C. Shuai, Y. Xu, P. Feng, G. Wang, S. Xiong, S. Peng, Antibacterial polymer scaffold based on mesoporous bioactive glass loaded with in situ grown silver, Chem. Eng. J. (2019) 304-315.

[11] M. Koller, Biodegradable and biocompatible polyhydroxy-alkanoates (PHA): auspicious microbial macromolecules for pharmaceutical and therapeutic applications, Molecules 23(2) (2018) 362/1-362/20.

[12] A. Kovalcik, S. Obruca, I. Fritz, I. Marova, Polyhydroxyalkanoates: Their Importance and Future, BioResources 14(2) (2019) 2468-2471.

[13] M. Koller, A review on established and emerging fermentation schemes for microbial production of Polyhydroxyalkanoate (PHA) biopolyesters, Fermentation 4(2) (2018) 30.

[14] C. Rigouin, S. Lajus, C. Ocando, V. Borsenberger, J.M. Nicaud, A. Marty, L. Avérous, F. Bordes, Production and characterization of two medium-chain-length polydroxyalkanoates by engineered strains of Yarrowia lipolytica, Microb. Cell Fact. 18(1) (2019) 99.

[15] K. Zhao, Y. Deng, J.C. Chen, G.-Q. Chen, Polyhydroxyalkanoate (PHA) scaffolds with good mechanical properties and biocompatibility, Biomaterials 24(6) (2003) 1041-1045.

[16] X.-Y. Xu, X.-T. Li, S.-W. Peng, J.-F. Xiao, C. Liu, G. Fang, K.C. Chen, G.-Q. Chen, The behaviour of neural stem cells on polyhydroxyalkanoate nanofiber scaffolds, Biomaterials 31(14) (2010) 3967-3975.

[17] A.C. Levine, A. Sparano, F.F. Twigg, K. Numata, C.T. Nomura, Influence of cross-linking on the physical properties and cytotoxicity of polyhydroxyalkanoate (PHA) scaffolds for tissue engineering, ACS Biomater. Sci. Eng. 1(7) (2015) 567-576.

[18] M. You, G. Peng, J. Li, P. Ma, Z. Wang, W. Shu, S. Peng, G.-Q. Chen, Chondrogenic differentiation of human bone marrow mesenchymal stem cells on polyhydroxyalkanoate (PHA) scaffolds coated with PHA granule binding protein PhaP fused with RGD peptide, Biomaterials 32(9) (2011) 2305-2313.

[19] S.-T. Cheng, Z.-F. Chen, G.-Q. Chen, The expression of cross-linked elastin by rabbit blood vessel smooth muscle cells cultured in polyhydroxyalkanoate scaffolds, Biomaterials 29(31) (2008) 4187-4194.

[20] Y.-W. Wang, Q. Wu, G.-Q. Chen, Reduced mouse fibroblast cell growth by increased hydrophilicity of microbial polyhydroxyalkanoates via hyaluronan coating, Biomaterials 24(25) (2003) 4621-4629.

[21] S. Rathbone, P. Furrer, J. Lübben, M. Zinn, S. Cartmell, Biocompatibility of polyhydroxyalkanoate as a potential material for ligament and tendon scaffold material, J. Biomed. Mater. Res. A 93(4) (2010) 1391-1403.

[22] E. Masaeli, P.A. Wieringa, M. Morshed, M.H. Nasr-Esfahani, S. Sadri, C.A. van Blitterswijk, L. Moroni, Peptide functionalized polyhydroxyalkanoate nanofibrous scaffolds enhance Schwann cells activity, Nanomedicine: Nanotechnology, Biology and Medicine 10(7) (2014) 1559-1569.

[23] T.H. Ying, D. Ishii, A. Mahara, S. Murakami, T. Yamaoka, K. Sudesh, R. Samian, M. Fujita, M. Maeda, T. Iwata, Scaffolds from electrospun polyhydroxyalkanoate copolymers: fabrication, characterization, bioabsorption and tissue response, Biomaterials 29(10) (2008) 1307-1317.

[24] T. Volova, D. Goncharov, A. Sukovatyi, A. Shabanov, E. Nikolaeva, E. Shishatskaya, Electrospinning of polyhydroxyalkanoate fibrous scaffolds: effects on electrospinning parameters on structure and properties, J. Biomat. Sci-Polym. E. 25(4) (2014) 370-393.

[25] D.-X. Wei, J.-W. Dao, G.-Q. Chen, A Micro-Ark for Cells: Highly Open Porous Polyhydroxyalkanoate Microspheres as Injectable Scaffolds for Tissue Regeneration, Adv. Mater. 30(31) (2018) 1802273.

[26] C. Mota, S.Y. Wang, D. Puppi, M. Gazzarri, C. Migone, F. Chiellini, G.Q. Chen, E. Chiellini, Additive manufacturing of poly [(R)-3-hydroxybutyrate-co-(R)-3-hydroxyhexanoate] scaffolds for engineered bone development, J. Tissue Eng. Regen. M. 11(1) (2017) 175-186.

[27] J.-Y. Baek, Z.-C. Xing, G. Kwak, K.-B. Yoon, S.-Y. Park, L.S. Park, I.-K. Kang, Fabrication and characterization of collagen-immobilized porous PHBV/HA nanocomposite scaffolds for bone tissue engineering, Journal of Nanomaterials 2012 (2012).

[28] S.A. Ashter, Introduction to Bioplastics Engineering, William Andrew Publishing, Oxford, UK, 2016.

[29] T. Pereira, M. Silva, M. Oliveira, I. Maia, J. Silva, M. Costa, R. Thiré, Effect of process parameters on the properties of selective laser sintered Poly (3-hydroxybutyrate) scaffolds for bone tissue engineering, Virtual and Physical Prototyping 7(4) (2012) 275-285.

[30] S. Saska, L.C. Pires, M.A. Cominotte, L.S. Mendes, M.F. de Oliveira, I.A. Maia, J.V.L. da Silva, S.J.L. Ribeiro, J.A. Cirelli, Three-dimensional printing and in vitro evaluation of poly(3-hydroxybutyrate) scaffolds functionalized with osteogenic growth peptide for tissue engineering, Mater. Sci. Eng. C 89 (2018) 265-273.

[31] B. Duan, W.L. Cheung, M. Wang, Optimized fabrication of Ca–P/PHBV nanocomposite scaffolds via selective laser sintering for bone tissue engineering, Biofabrication 3(1) (2011) 015001.

[32] S.H. Diermann, M. Lu, G. Edwards, M. Dargusch, H. Huang, In vitro degradation of a unique porous PHBV scaffold manufactured using selective laser sintering, J. Biomed. Mater. Res. A 107(1) (2019) 154-162.

[33] W. Kosorn, M. Sakulsumbat, P. Uppanan, P. Kaewkong, S. Chantaweroad, J. Jitsaard, K. Sitthiseripratip, W. Janvikul, PCL/PHBV blended three dimensional scaffolds fabricated by fused

deposition modeling and responses of chondrocytes to the scaffolds, J. Biomad. Mater. Res. B 105(5) (2017) 1141-1150.

[34] R. Kudelski, J. Cieslik, M. Kulpa, P. Dudek, K. Zagorski, R. Rumin, Comparison of cost, material and time usage in FDM and SLS 3D printing methods, 2017 XIIIth International Conference on Perspective Technologies and Methods in MEMS Design (MEMSTECH), IEEE, 2017, pp. 12-14.

[35] A. Kovalcik, K. Meixner, M. Mihalic, W. Zeilinger, I. Fritz, W. Fuchs, P. Kucharczyk, F. Stelzer, B. Drosg, Characterization of polyhydroxyalkanoates produced by Synechocystis salina from digestate supernatant, Int. J. Biol. Macromol. 102 (2017) 497-504.

[36] I. Zein, D.W. Hutmacher, K.C. Tan, S.H. Teoh, Fused deposition modeling of novel scaffold architectures for tissue engineering applications, Biomaterials 23(4) (2002) 1169-1185.

[37] J.G. Ausejo, J. Rydz, M. Musioł, W. Sikorska, M. Sobota, J. Włodarczyk, G. Adamus, H. Janeczek, I. Kwiecień, A. Hercog, A comparative study of three-dimensional printing directions: The degradation and toxicological profile of a PLA/PHA blend, Polym. Degrad. Stabil. 152 (2018) 191-207.

[38] ColorFabb, Filaments PLA/PHA value pack, 2018. (Accessed 01.11.2018 2018).

[39] P. Research, Filament PLA/PHA, 2019. (Accessed 01.07.2019).

[40] S. Wang, L. Capoen, D.R. D'hooge, L. Cardon, Can the melt flow index be used to predict the success of fused deposition modelling of commercial poly (lactic acid) filaments into 3D printed materials?, Plastics, Rubber and Composites 47(1) (2018) 9-16.

[41] A.F. Balogová, R. Hudák, T. Tóth, M. Schnitzer, J. Feranc, D. Bakoš, J. Živčák, Determination of geometrical and viscoelastic properties of PLA/PHB samples made by additive manufacturing for urethral substitution, J. Biotechnol. 284 (2018) 123-130.

[42] I. Armentano, E. Fortunati, N. Burgos, F. Dominici, F. Luzi, S. Fiori, A. Jiménez, K. Yoon, J. Ahn, S. Kang, Processing and characterization of plasticized PLA/PHB blends for biodegradable multiphase systems, Express Polym. Lett. 9 (7) (2015) 583-596.

[43] J.V. Ecker, I. Burzic, A. Haider, S. Hild, H. Rennhofer, Improving the impact strength of PLA and its blends with PHA in fused layer modelling, Polym. Test. 78 (2019) 105929.

[44] A.T. Lorenzo, M.L. Arnal, J.J. Sánchez, A.J. Müller, Effect of annealing time on the self-nucleation behavior of semicrystalline polymers, J. Polym. Sci. Pol. Phys. 44(12) (2006) 1738-1750.

[45] T.W. Atkins, S.J. Peacock, In vitro biodegradation of polyhydroxybutyrate-hydroxyvalerate microcapsules exposed to Hank's buffer, newborn calf serum, pancreatin and synthetic gastric juice, J. Microencapsul. 14(1) (1997) 35-49.

[46] A.J. Müller, M. Ávila, G. Saenz, J. Salazar, Crystallization of PLA-based Materials, in: A. Jiménez, M.A. Peltzer, R.A. Ruseckaite (Eds.), Poly(lactic acid) Science and Technology: Processing, Properties, Additives and Applications, RSC Polymer Chemistry Series, Cambridge, 2015, pp. 66-98.

[47] A. Greco, A. Maffezzoli, Rotational moulding of poly-lactic acid, AIP Conference Proceedings, AIP Publishing, 2016, p. 060007.

[48] P. Barham, A. Keller, E. Otun, P. Holmes, Crystallization and morphology of a bacterial thermoplastic: poly-3-hydroxybutyrate, J. Mater. Sci. 19(9) (1984) 2781-2794.

[49] E. Ten, Jiang, L, Zhang, J., Wolcott, M.P., Mechanical performance of polyhydroxylalkanoates (PHA)-based biocomposites, in: M. Misra, Pandey, J.K., Mohanty, A. (Ed.), Biocomposites: Design and Mechanical Performance, Elsevier Science, Cambridge UK, 2015, p. 39.

[50] M. Safari, A. Mugica, M. Zubitur, A. Martínez de Ilarduya, S. Muñoz-Guerra, A.J. Müller, Controlling the Isothermal Crystallization of Isodimorphic PBS-ran-PCL Random Copolymers by Varying Composition and Supercooling, Polymers 12(1) (2020) 17.

[51] P. Xu, Y. Cao, P. Lv, P. Ma, W. Dong, H. Bai, W. Wang, M. Du, M. Chen, Enhanced crystallization kinetics of bacterially synthesized poly(3-hydroxybutyrate-co-3-hydroxyhexanate) with structural optimization of oxalamide compounds as nucleators, Polym. Degrad. Stabil. 154 (2018) 170-176.

[52] S.J. Organ, P.J. Barham, On the equilibrium melting temperature of polyhydroxybutyrate, Polymer 34(10) (1993) 2169-2174.

[53] S.J. Organ, Variation in melting point with molecular weight for hydroxybutyrate/hydroxyvalerate copolymers, Polymer 34(10) (1993) 2175-2179.

[54] P. Holcapkova, P. Stloukal, P. Kucharczyk, M. Omastova, A. Kovalcik, Anti-hydrolysis effect of aromatic carbodiimide in poly(lactic acid)/wood flour composites, Compos. Part A-Appl. S. 103 (2017) 283-291.

[55] S.K. Misra, S.P. Valappil, I. Roy, A.R. Boccaccini, Polyhydroxyalkanoate (PHA)/inorganic phase composites for tissue engineering applications, Biomacromolecules 7(8) (2006) 2249-2258.

[56] Z. Mo, J. Lin, X. Zhang, Y. Fan, X. Xu, Y. Xue, D. Liu, J. Li, L. Hu, C. Tang, Morphology controlled synthesis zinc oxide and reinforcement in polyhydroxyalkanoates composites, Polym. Composites 35(9) (2014) 1701-1706.

[57] N. Pramanik, J. De, R.K. Basu, T. Rath, P.P. Kundu, Fabrication of magnetite nanoparticle doped reduced graphene oxide grafted polyhydroxyalkanoate nanocomposites for tissue engineering application, RSC Adv. 6(52) (2016) 46116-46133.

[58] P. Feng, Y. Kong, L. Yu, Y. Li, C. Gao, S. Peng, H. Pan, Z. Zhao, C. Shuai, Molybdenum disulfide nanosheets embedded with nanodiamond particles: co-dispersion nanostructures as reinforcements for polymer scaffolds, Appl. Mater. Today 17 (2019) 216-226.

[59] C. Shuai, W. Guo, P. Wu, W. Yang, S. Hu, Y. Xia, P. Feng, A graphene oxide-Ag co-dispersing nanosystem: dual synergistic effects on antibacterial activities and mechanical properties of polymer scaffolds, Chem. Eng. J. 347 (2018) 322-333.

[60] X. Yang, K. Zhao, G.-Q. Chen, Effect of surface treatment on the biocompatibility of microbial polyhydroxyalkanoates, Biomaterials 23(5) (2002) 1391-1397.
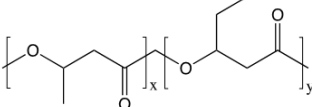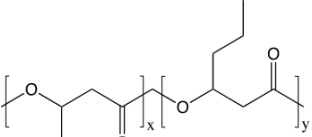
[61] Y.Y. Shangguan, Y.W. Wang, Q. Wu, G.Q. Chen, The mechanical properties and in vitro biodegradation and biocompatibility of UV-treated poly(3-hydroxybutyrate-co-3-hydroxyhexanoate), Biomaterials 27, (2006) 2349-2357.

[62] H.-X. Yang, M. Sun, Y. Zhang, P. Zhou, Degradable PHBHHx modified by the silk fibroin for the applications of cardiovascular tissue engineering, ISRN Materials Science 2011, ID 389872, (2011).

[63] C. Shuai, Y. Cheng, W. Yang, P. Feng, Y. Yang, C. He, F. Qi, S. Peng, Magnetically actuated bone scaffold: Microstructure, cell response and osteogenesis, Compos Part B-Eng. (2020) 107986.

[64] L. Avérous, Synthesis, Properties, Environmental and Biomedical Applications of Polylactic Acid, in: S. Ebnesajjad (Ed.), Handbook of Biopolymers and Biodegradable Plastics: Properties, Processing and Applications, Elsevier Science, Oxford, UK, 2013, p. 181.

[65] B. Laycock, M. Nikolić, J.M. Colwell, E. Gauthier, P. Halley, S. Bottle, G. George, Lifetime prediction of biodegradable polymers, Prog. Polym. Sci. 71 (2017) 144-189.

[66] A. Bonartsev, A. Boskhomodgiev, A. Iordanskii, G. Bonartseva, A. Rebrov, T. Makhina, V. Myshkina, S. Yakovlev, E. Filatova, E. Ivanov, Hydrolytic degradation of poly (3-hydroxybutyrate), polylactide and their derivatives: kinetics, crystallinity, and surface morphology, Mol. Cryst. Liq. Cryst. 556(1) (2012) 288-300.

Table 1

Molecular weight, polydispersity and melt volume rates (MVR) of polymers.

Sample		M_n (kDa)	M_w (kDa)	Đ	MVR at 190°C, 2.16 kg (cm^3 10 min^{-1})
PLA 2003D		85 ± 2	98 ± 2	1.15	13.3 ± 1
PHB Hydal		299 ± 3	350 ± 3	1.17	nd

20

PHBV, Mirel P1004			105 ± 3	290 ± 4	2.76	108.9 ± 3
PHBH X131A			121 ± 1	163 ± 4	1.35	18.3 ± 2

nd – not determined

Table 2

Conditions for isothermal crystallization kinetics study by DSC; T_c – crystallization temperature.

Sample	1st step	2nd step	3rd step	4th step	5th step
PHB	Heating $25 \rightarrow 190\,°C$ at 20 °C min^{-1}	Holding 3 min at 190 °C	Cooling $190\,°C \rightarrow T_c$ at 60 °C min^{-1} $T_c = 81 - 89\,°C$	Holding step for enough time to allow the sample to complete isothermal crystallization	Heating $T_c \rightarrow 190\,°C$ at 20 °C min^{-1} in order to record the melting behavior after the isothermal crystallization
PHBV	Heating $25 \rightarrow 165\,°C$ at 20 °C min^{-1}	Holding 3 min at 190 °C	Cooling $190\,°C \rightarrow T_c$ at 60 °C min^{-1} $T_c = 117 - 128\,°C$	Holding step for enough time to allow the sample to complete isothermal crystallization	Heating $T_c \rightarrow 190\,°C$ at 20 °C min^{-1} in order to record the melting behavior after the isothermal crystallization
PHBH	Heating $25 \rightarrow 165\,°C$ at 20°C min^{-1}	Holding 3 min at 190 °C	Cooling $165\,°C \rightarrow T_c$ at 60 °C min^{-1} $T_c = 106 - 117\,°C$	Holding step for enough time to allow the sample to complete isothermal crystallization	Heating $T_c \rightarrow 165\,°C$ at 20 °C min^{-1} in order to record the melting behavior after the isothermal crystallization

Table 3

Differential scanning calorimetry data of PLA and PHAs.

	1st heating cycle		Cooling cycle			2nd heating cycle			
Sample	T_m (°C)	ΔH_m (J g^{-1})	T_c (°C)	ΔH_c (J g^{-1})	T_g (°C)	T_{cc} (°C)	ΔH_{cc} (J g^{-1})	T_m (°C)	ΔH_m (J g^{-1})

21

PLA	151.1	34.4	-	-	61.7	-	-	-	-
PHB	169.3	63.8	41.1	7.8	-10.2	46.4	26.4	163.7	66.9
PHBV	148.9/169.4	32.8	101.9	36.1	-7.8	-	-	155.8/167.8	30.6
PHBH	134.7/144.4	27.2	82.9	43.4	0.7	-	-	134.5/144.9	29.0

Table 4

Parameters of the Avrami fit obtained from the isothermal crystallization at different crystallization temperatures (T_c).

Sample		Avrami parameters					Melting behavior after isothermal crystallization			
	T_c (°C)	n	$t_{1/2\ theo}$ (min)	$t_{1/2\ exp}$ (min)	k (min^{-1})	R^2	T_{m1} (°C)	ΔH_{m1} (J g^{-1})	T_{m2} (°C)	ΔH_{m2} (J g^{-1})
PHB										
	82	2.2	3.12	2.77	0.05440	0.9987	152.0	14.0	165.2	31.0
	83	2.6	3.58	3.36	0.02620	0.9989	151.5	13.6	165.2	30.7
	85	2.8	6.21	6.68	0.00431	0.9999	151.5	19.4	164.3	29.0
	86	3.2	7.40	7.61	0.00120	0.9995	151.6	17.5	164.1	30.0
	87	3.3	9.96	9.96	0.00038	0.9984	151.6	16.7	164.1	29.2
	88	3.5	7.24	7.47	0.00063	0.9990	151.0	18.5	163.7	28.2
	89	4.1	8.49	9.49	0.00010	0.9949	150.9	18.7	163.5	27.5
PHBV	117	2.9	0.91	0.90	0.90900	0.9999	159.9	26.6	166.9	3.0
	118	3.1	1.06	1.06	0.57500	0.9999	159.2	26.8	166.5	2.5
	119	2.9	1.18	1.17	0.43300	0.9999	158.7	27.1	166.0	2.0
	120	3.7	1.53	1.57	0.14200	1.0000	157.2	26.6	165.4	1.5
	121	3.6	1.83	1.87	0.07940	1.0000	156.6	26.8	164.4	1.4
	122	3.8	2.26	2.33	0.03210	1.0000	156.1	25.7	164.1	1.2
	123	3.8	2.81	2.91	0.01350	0.9999	155.6	25.6	163.3	0.3
	124	3.5	3.33	3.44	0.01020	1.0000	155.3	24.7	-	-
	125	4.2	4.52	4.75	0.00129	0.9998	155.0	23.2	-	-
	127	4.1	7.63	8.03	0.00017	0.9999	154.6	21.0	-	-
	128	4.3	10.1	10.64	0.00003	0.9999	154.4	20.9	-	-
PHBH	107	3.4	3.06	3.06	0.01510	0.9998	140.1	32.8	-	-
	108	3.5	3.44	3.42	0.00936	0.9998	140.4	33.4	-	-
	109	3.5	3.82	3.79	0.00631	0.9998	140.5	33.4	-	-
	110	3.5	4.37	4.34	0.00375	0.9997	140.8	33.7	-	-
	111	3.5	4.87	4.82	0.00270	0.9997	141.3	34.4	-	-
	112	3.4	5.42	5.34	0.00210	0.9997	141.7	35.2	-	-
	113	3.5	6.13	6.10	0.00120	0.9998	142.2	36.0	-	-
	114	3.5	6.94	6.84	0.00077	0.9997	142.5	37.1	-	-
	115	3.3	7.45	7.83	0.00098	0.9995	142.9	38.2	-	-
	116	3.5	8.95	8.84	0.00030	0.9996	143.3	39.5	-	-
	117	3.7	10.62	10.51	0.00010	0.9996	143.6	40.7	-	-

22

n- Avrami exponent, predicted half-time crystallization ($t_{1/2\ theo}$), experimental half-time crystallization ($t_{1/2\ exp}$), overall transformation constant (k) and the data correlation coefficient (R^2)

Table 5

TGA data of PLA, PHB, PHBV and PHBH in air and at heating rate of 10°C min^{-1}.

Sample	T_{onset} (°C)	T_{max} (°C)	$Mass_{rest}$ at 500°C (%)
PLA	282.0	339.6	0
PHB	243.1	276.2	0
PHBV	230.1	286.8 and 352.8	2.8
PHBH	250.9	276.9 and 318.0	0

Table 6

Newtonian viscosities of PLA pellets and PHAs pellets after multiple frequency sweeps at selected temperatures.

Number of runs	η_0 (Pa s) at 1 Hz			
	PLA at 185 °C	PHB at 175 °C	PHBV at 175 °C	PHBH at 150 °C
1st run	213.8	1500	51.0	7609
2nd run	209.5	1305	45.0	7423
3rd run	206.7	1100	39.3	7052

Table 7

Mechanical properties of PLA and PHBH filaments (fil) and scaffolds (scaf).

Sample	E (MPa)	σ_B (MPa)	ε_B (%)
PLA_fil	670 ± 17.1	46.2 ± 1.6	24 ± 2.6
PHBH_fil	260 ± 28.0	22.1 ± 4.0	22 ± 4.0
PLA_scaf	1510 ± 23.7	30.4 ± 1.7	16 ± 0.5
PHBH_scaf	960 ± 80.0	18.3 ± 2.5	11 ± 0.9

23

Table 8

DMA properties of PLA and PHBH scaffolds.

Sample	Storage modulus, E′ (MPa) at					Loss factor, Tan δ			
	-20 °C	0 °C	20 °C	37 °C	60 °C	Tan δ_1 at max	Tan δ_1 at max (°C)	Tan δ_2 at max	Tan δ_2 at max (°C)
PLA_scaf	2630	2460	2140	1580	10	1.84	53.2	-	-
PHBH_scaf	3870	3560	1740	1030	590	0.13	15.8	0.07	58.2

Table 9
Abiotic hydrolysis of biopolymers *in vitro* at 37 °C in synthetic gastric juice, scaffolds of 35×21×0.34 mm.

Incubation time (days)	Relative mass change related to the original weight (%)	M_w (kDa)	Đ	Relative decrease of M_w (%)
PLA				
0	0	101 ± 3.32	1.54 ± 0.49	0
6	+ 6.03 ± 1.12	90 ± 3.14	1.53 ± 0.11	10.9
20	+ 7.13 ± 0.45	77 ± 4.90	1.52 ± 0.07	23.8
40	- 0.18 ± 0.08	63 ± 1.67	1.62 ± 0.09	37.6
52	- 1.16 ± 0.15	57 ± 1.03	1.51 ± 0.10	43.6
PHBH				
0	0	162 ± 3.46	1.31 ± 0.07	0
6	+ 1.82 ± 0.65	109 ± 5.87	1.51 ± 0.09	32.6
20	+ 1.77 ± 0.74	92 ± 0.09	1.45 ± 0.01	42.8
40	- 0.08 ± 0.03	68 ± 1.19	1.46 ± 0.03	57.9
52	- 0.31 ± 0.08	61 ± 1.73	1.62 ± 0.10	62.7

Table 10

Thermal characteristics derived from first DSC heating scan.

Sample	T_{cc1} (°C)	ΔH_{cc1} (J g^{-1})	T_{cc2} (°C)	ΔH_{cc2} (J g^{-1})	T_{m1} (°C)	T_{m2} (°C)	T_{m3} (°C)	ΔH_m (J g^{-1})	$^a X_c$ (%)
PLA_scaf_0 days	88.1	20.5	137.1	1.8	149.2			25.2	3.1
PLA_scaf_52 days	-	-	-	-	151.5			27.2	29.2
PHBH_scaf_0 days	-	-	114.0	2.8	124.6	144.4	154.3	33.3	-
PHBH_scaf_52 days	-	-	-	-	125.5	142.7	151.2	35.2	-

$^a X_c = \frac{\Delta H_m - \Delta H_{cc}}{\Delta H_m^0} \times 100$, ΔH_m^0 of PLA = 93.0 J g^{-1} [39]
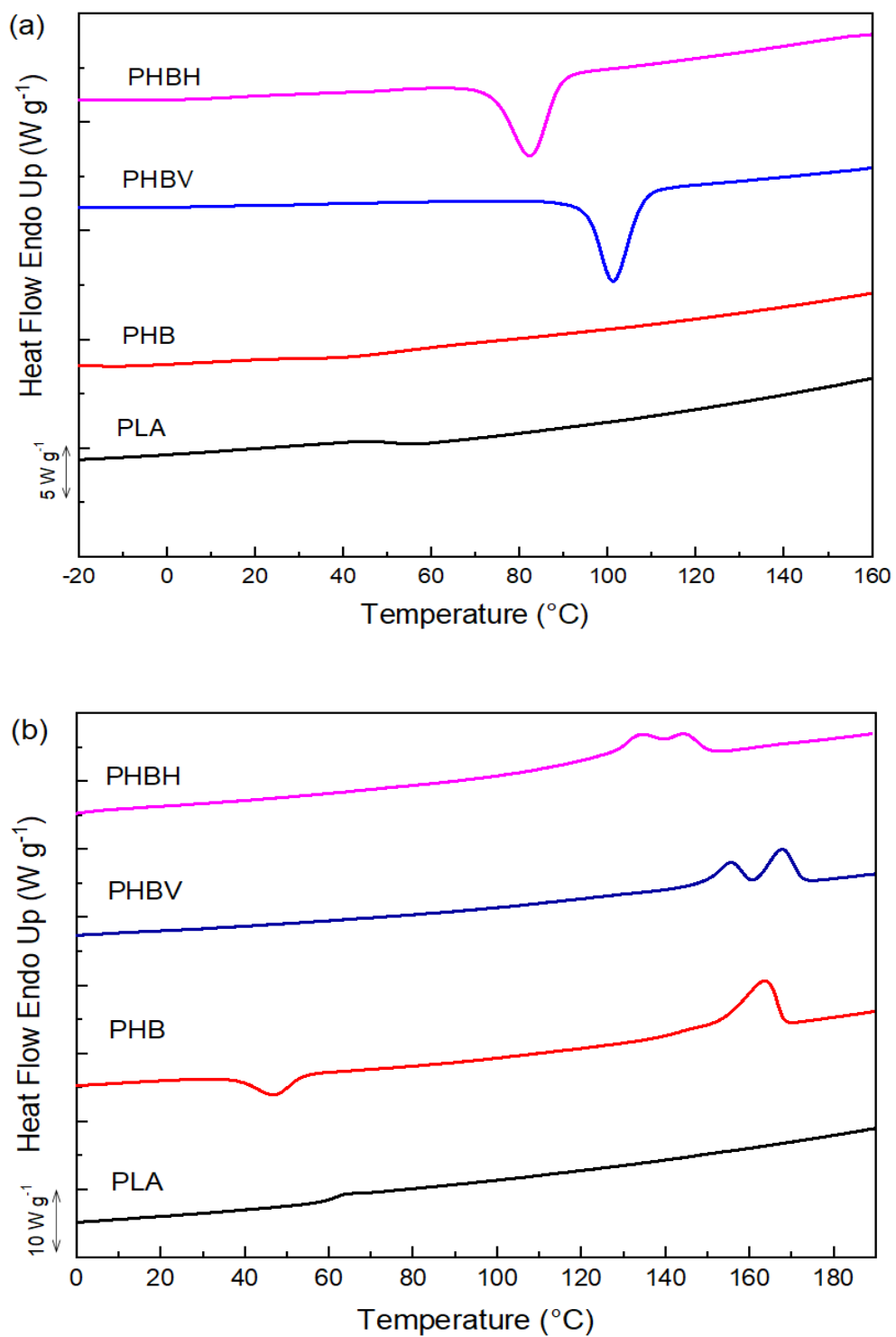
Fig. 1. DSC (a) cooling and (b) subsequent heating scans for PLA, PHB, PHBV and PHBH. [Color Figure can be viewed in the online issue].
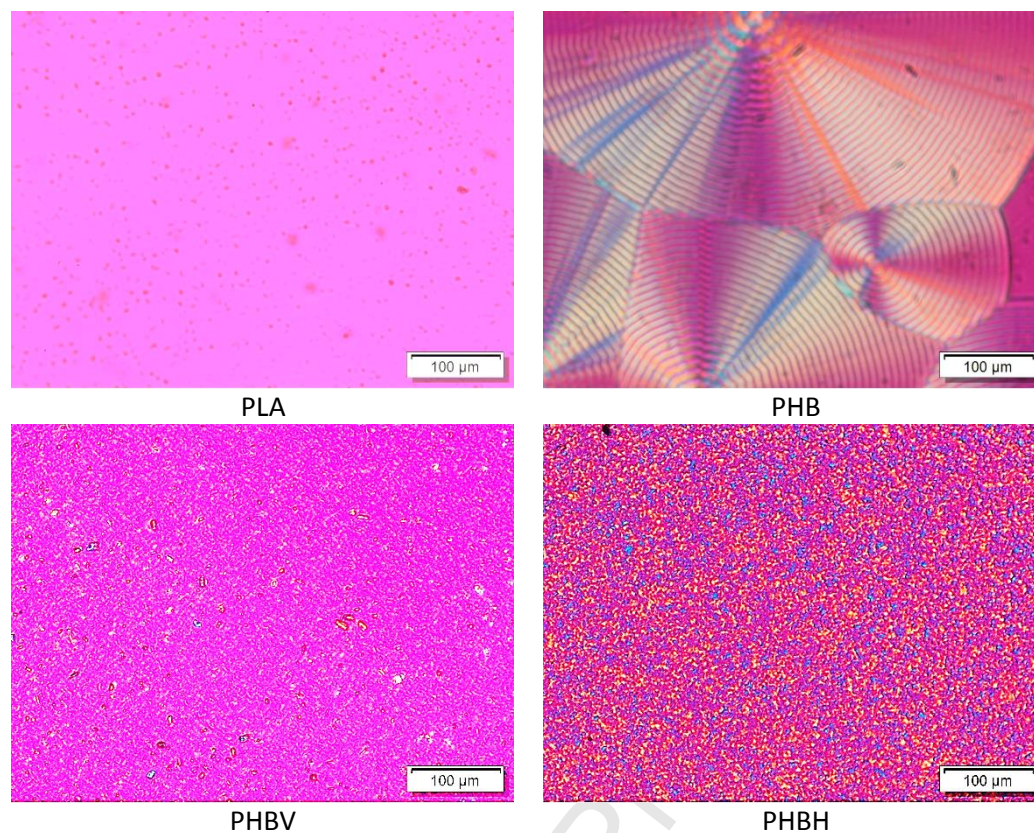
Fig. 2. Polarized Light Optical Micrographs of spherulitic morphology of poly(lactic acid) (PLA) and polyhydroxyalkanoates (PHB, PHBH, and PHBV). Micrographs have been taken at room temperature after cooling from the melt at 20°C min^{-1}. [Color Figure can be viewed in the online issue].
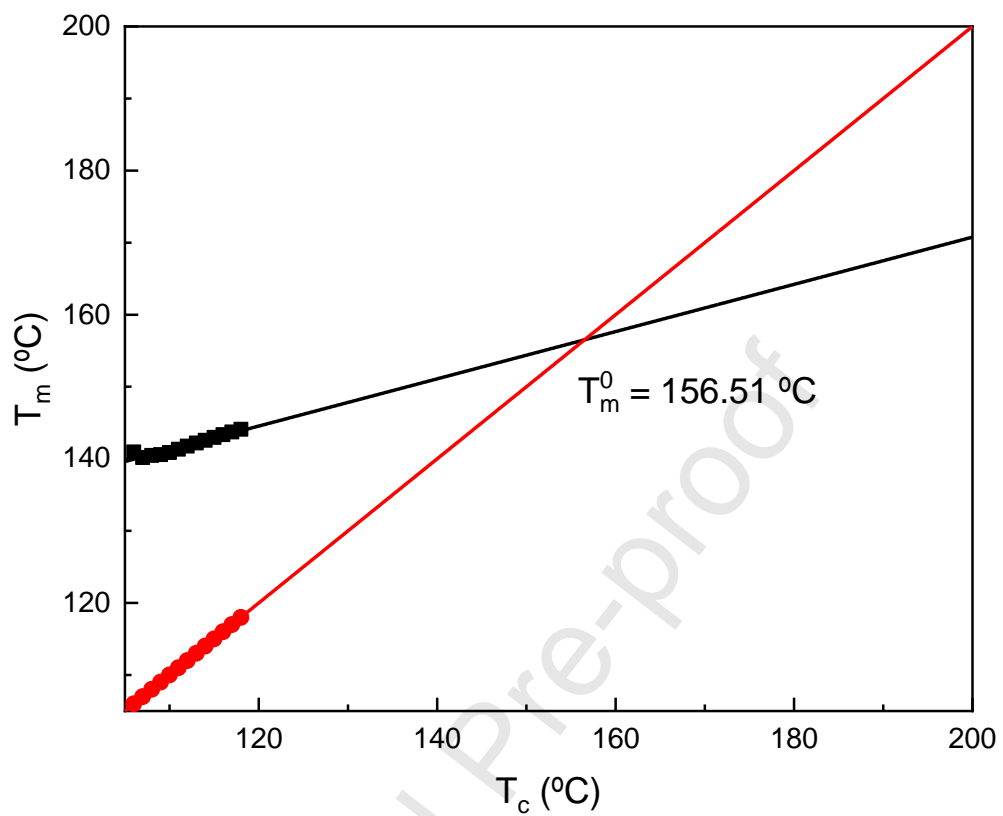
Fig. 3. Hoffman-Weeks plot for determination of T_m^0 of PHBH. [Color Figure can be viewed in the online issue].
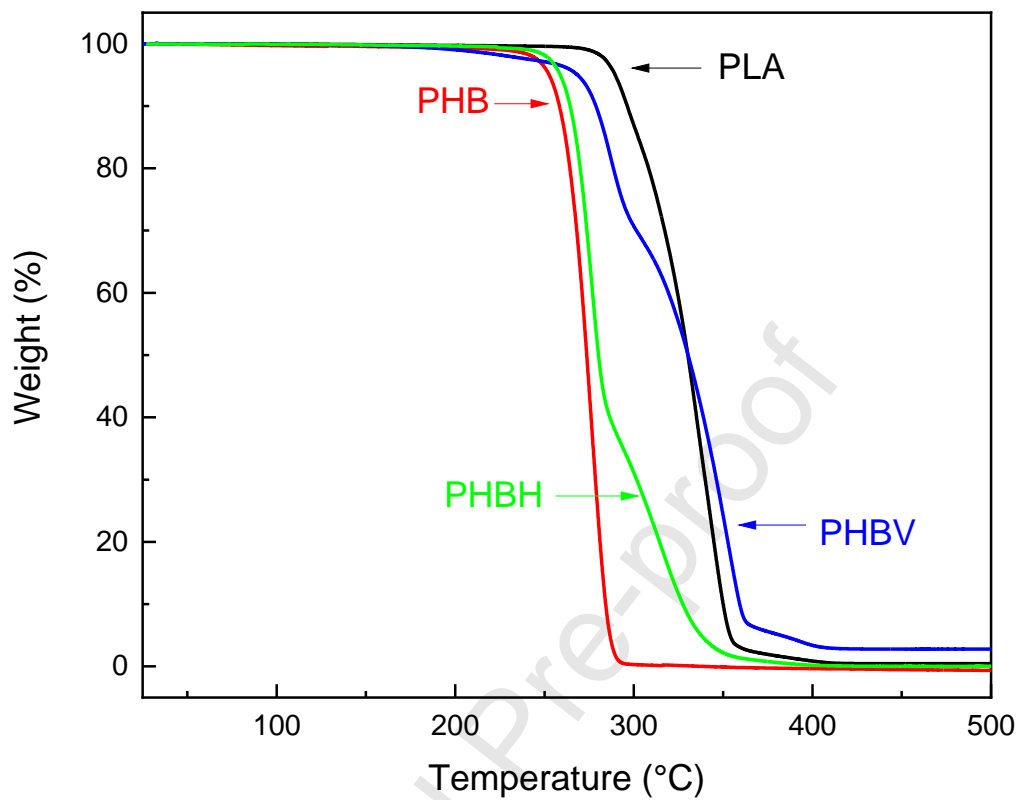
Fig. 4. Weight of the samples as a function of temperature obtained by TGA for PLA, PHB, PHBV and PHBH. [Color Figure can be viewed in the online issue].
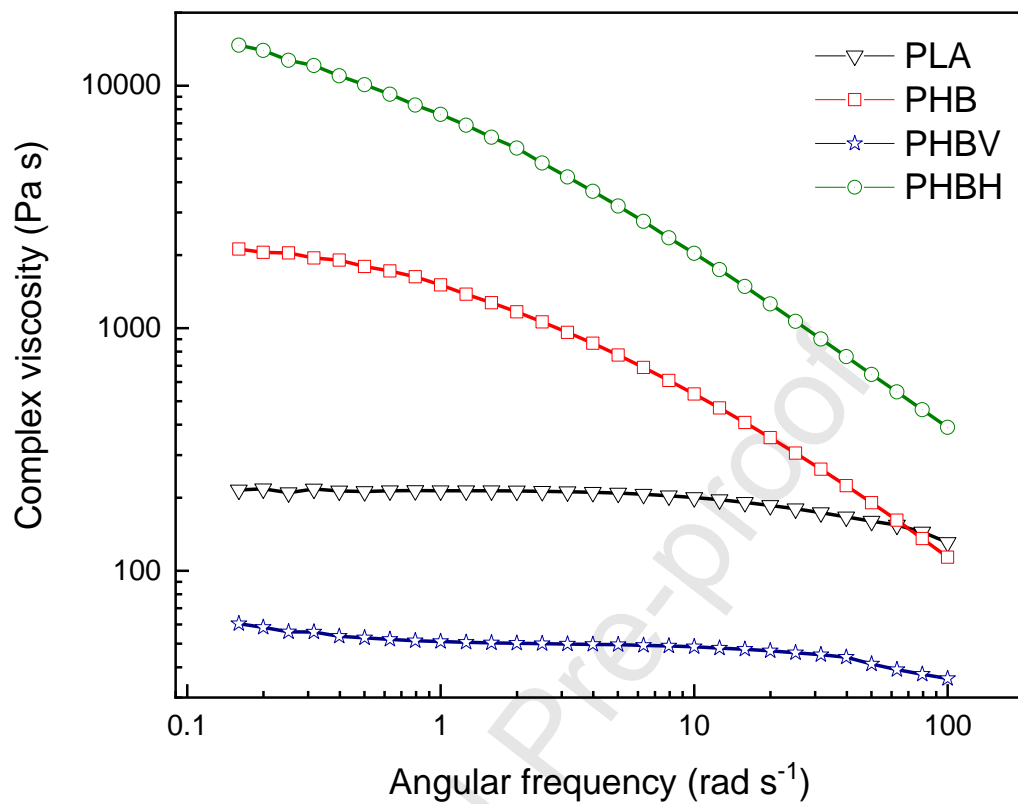
Fig. 5. Plots of complex viscosity versus frequency for PLA, PHAs at processing temperatures used for filament extrusion. [Color Figure can be viewed in the online issue].
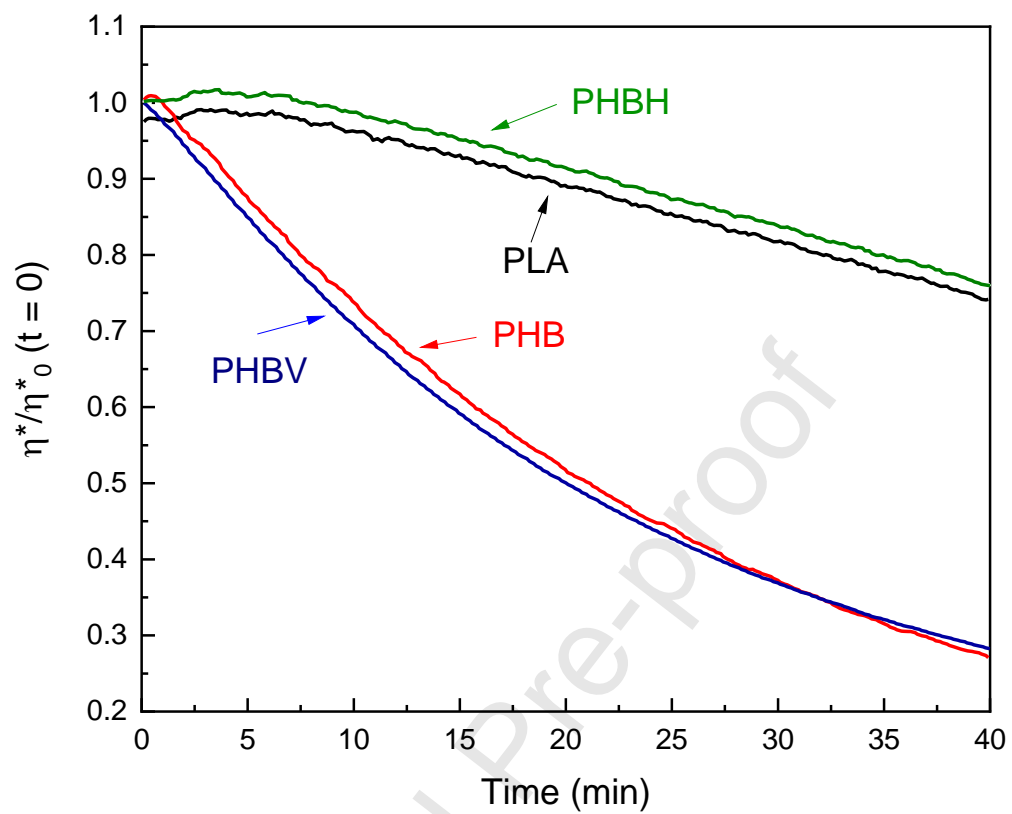
Fig. 6. Evolution of complex viscosity, η^* (t)/ η^*_0 (t=0) versus time of PLA, PHB, PBHV and PHBH. [Color Figure can be viewed in the online issue].
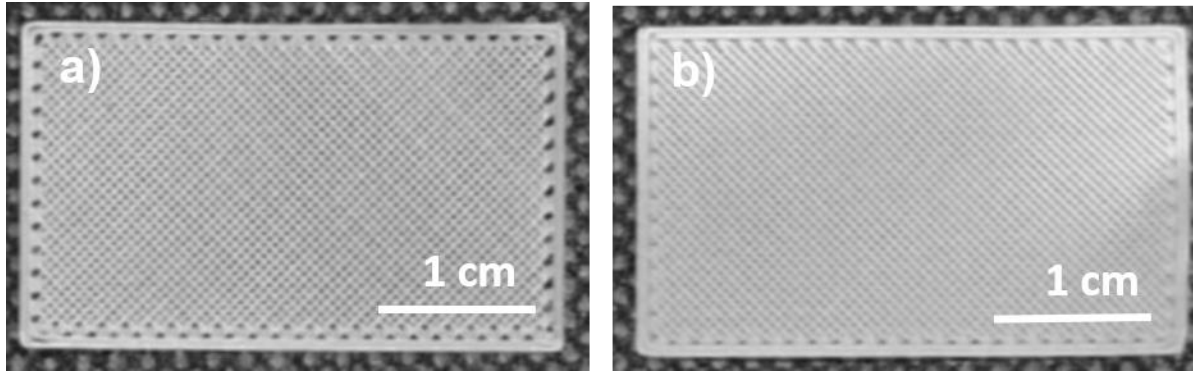
Fig. 7. 3D printed (a) PHBH scaffolds and (b) PLA scaffolds. [Color Figure can be viewed in the online issue].
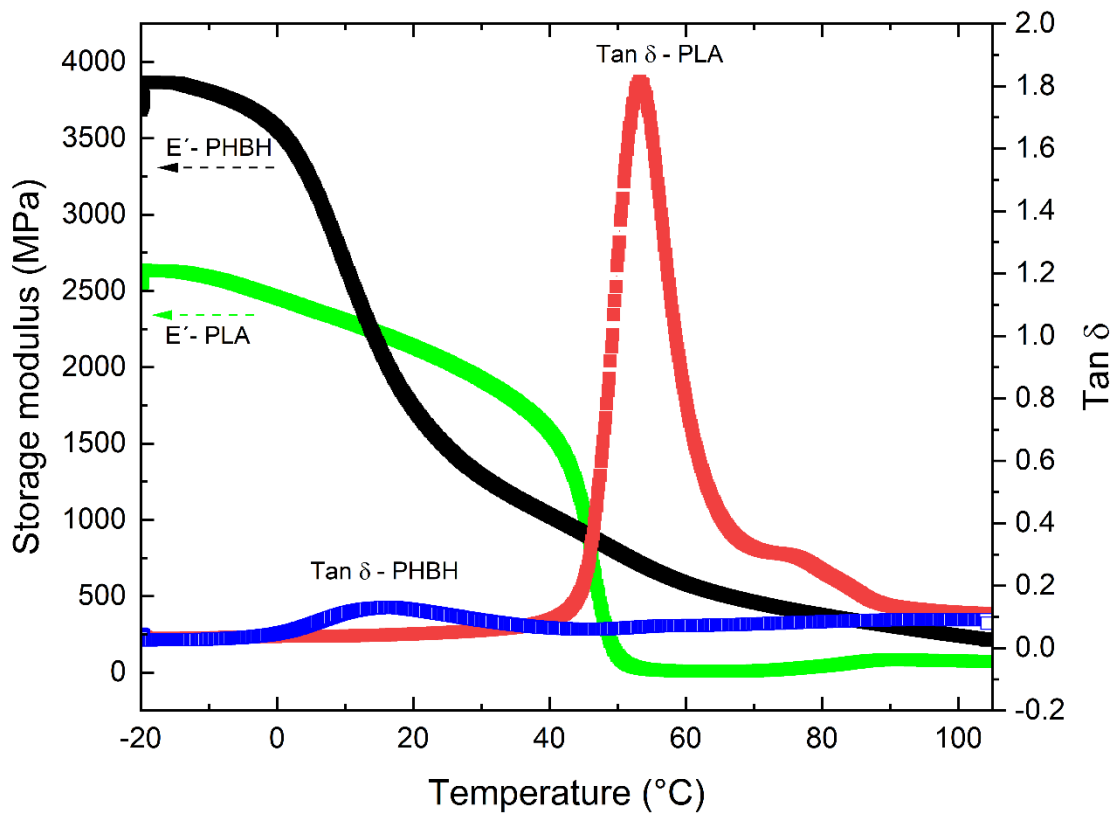

Fig. 8. Temperature dependence of storage moduli and loss factors of PLA and PHBH scaffolds. [Color Figure can be viewed in the online issue].
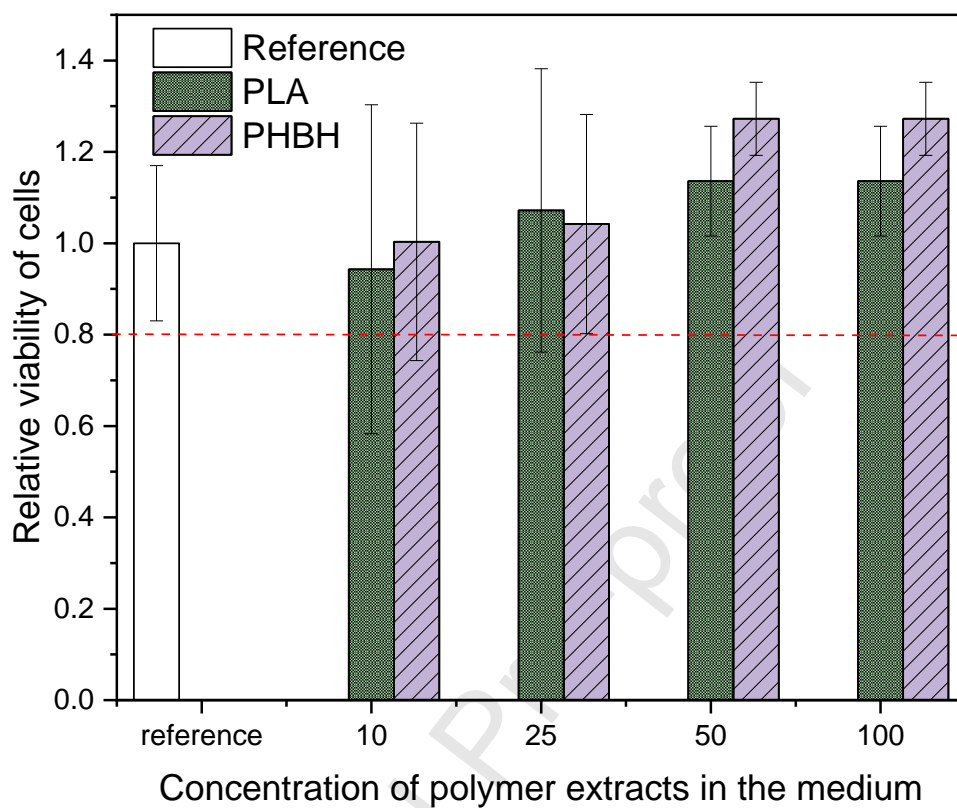
Fig. 9. Relative number of viable cells compared to reference according to ISO 10993-5 standard. The dashed line highlights the critical viability to be assessed according to requirements of EN ISO 10993-5, where viability > 0.8 means no cytotoxicity. [Color Figure can be viewed in the online issue].
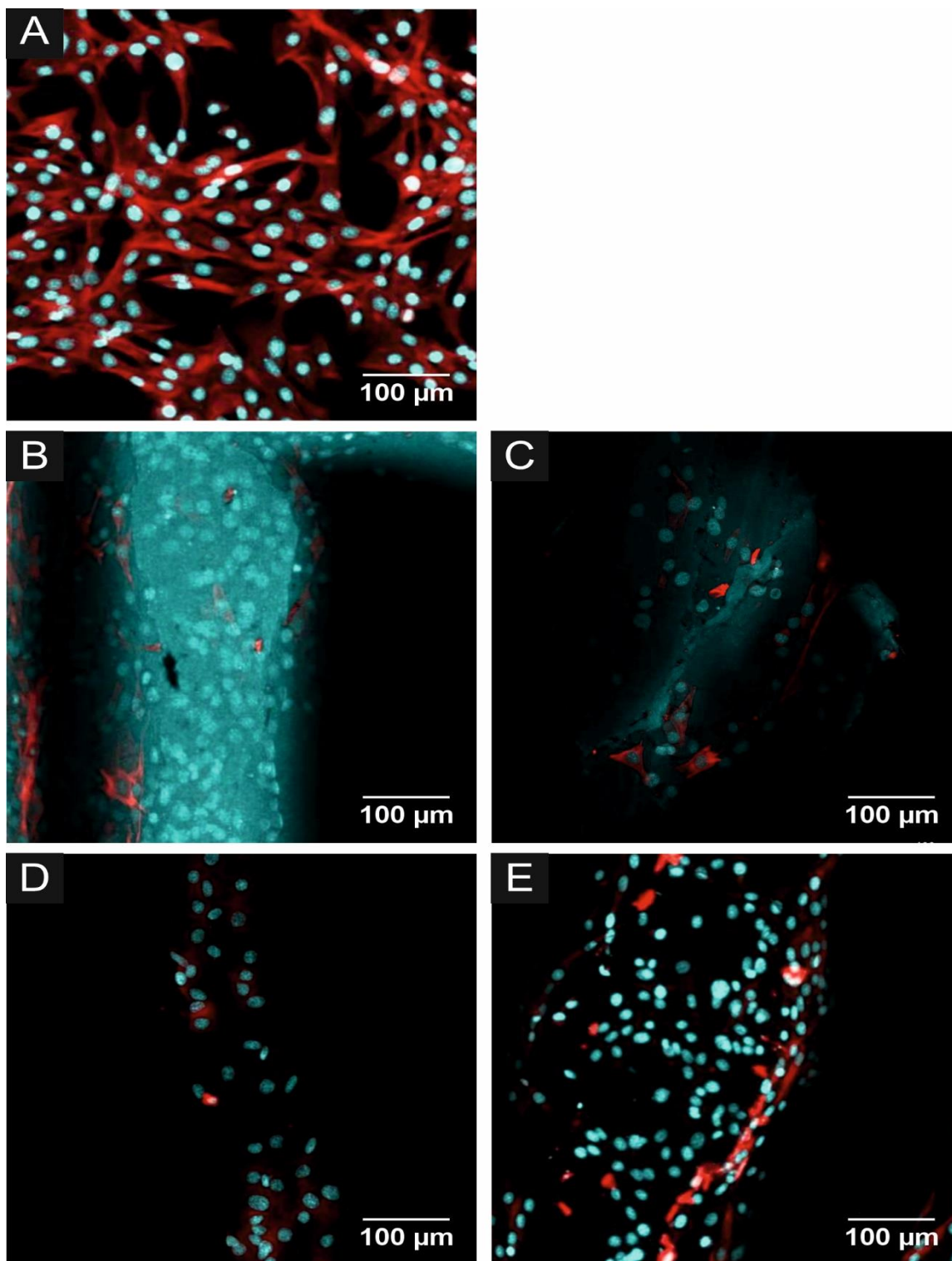
Fig. 10. Micrographs of NIH/3T3 cultivated directly on PLA and PHBH scaffolds. A) Reference; B) PLA; C) PLA coated with gelatine; D) PHBH; E) PHBH coated with gelatine. [Color Figure can be viewed in the online issue].
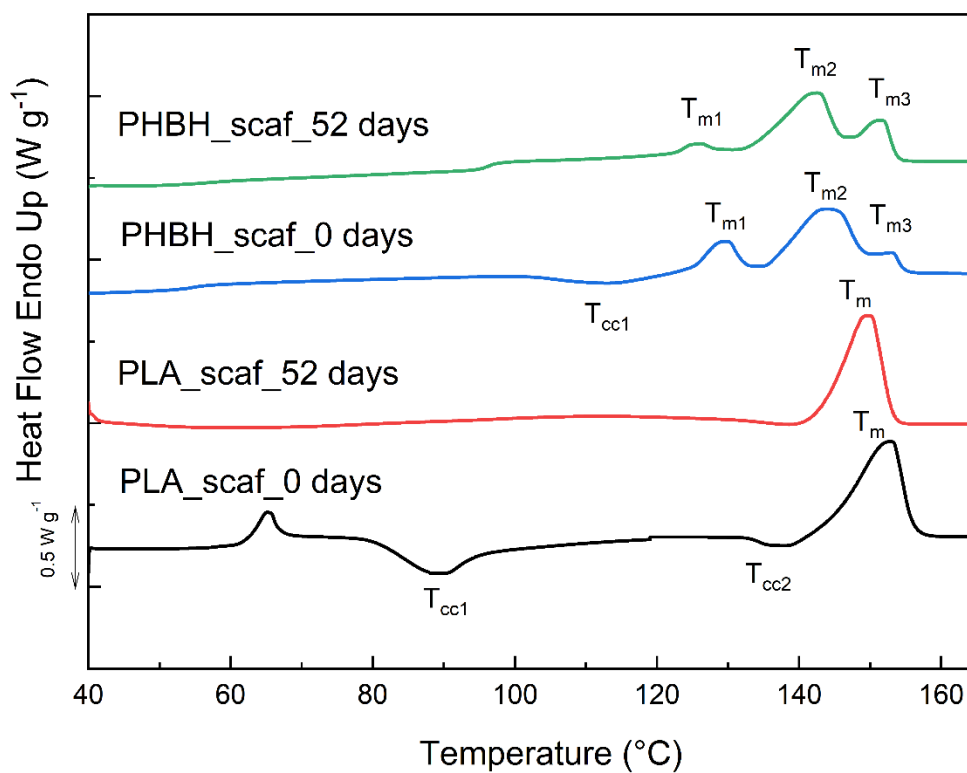
Fig. 11. DSC first heating scans of scaffolds before (0 days) and after abiotic degradation (52 days) in the synthetic gastric juice. [Color Figure can be viewed in the online issue].
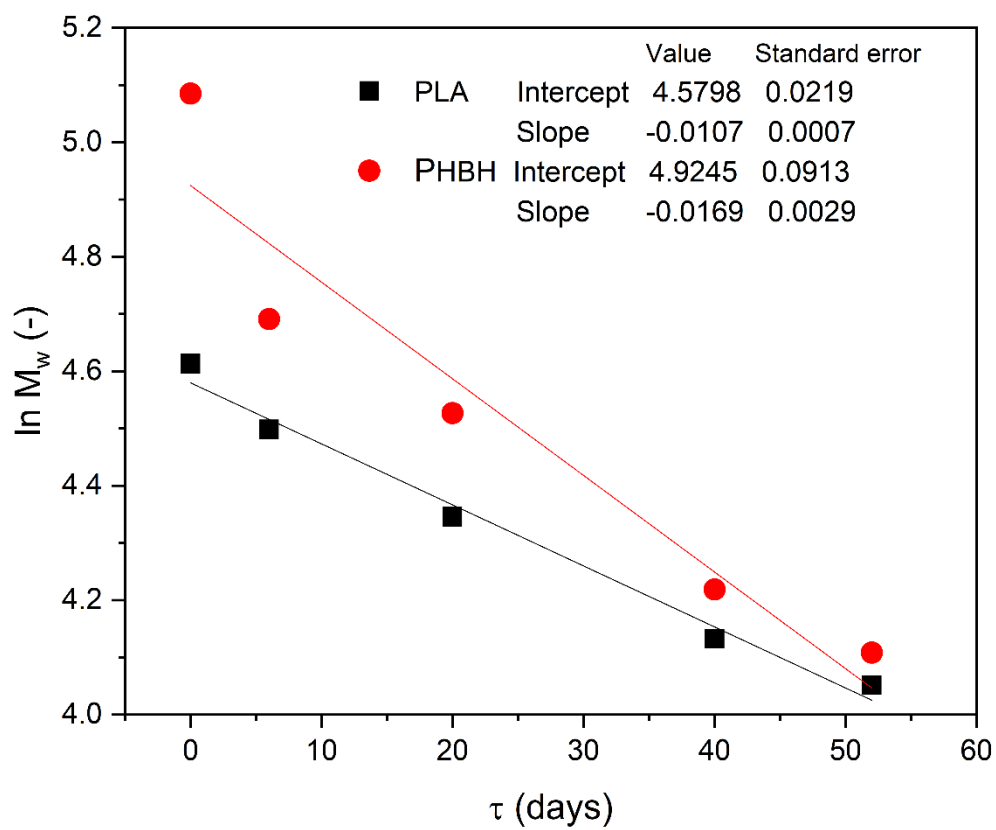
Fig. 12. Linearized model of first-order kinetics applied on degradation of PHBH and PLA. [Color Figure can be viewed in the online issue].

Author contributions

Conceptualization, A.K.; Methodology, A.K. and A.J.M.; Investigation, A.K., L.S., M.K., K.S., and M.O., Formal analysis, A.K., L.S., M.K., and P.H.; Visualization, A.K., L.S., P.H., and M.K.; Resources, A.K.; Writing-original draft preparation and review, A.K. and A.J.M.; Writing - review and editing, L.S., M.K., P.H., M.O., and N.M. All authors have read and agreed to the published version of the manuscript.

Graphical abstract

Highlights
- PHBH displayed thermal stability and rheological properties comparable with PLA
- PHBH scaffolds were prepared by fused deposition modeling
- PHBH scaffolds displayed remarkable mechanical and viscoelastic properties
- PHBH scaffolds were non-toxic and supported excellent cells proliferation
- Satisfactory degradation rate of PHBH and PLA scaffolds in synthetic gastric juice